

The separation of CO₂ from ambient air – A techno-economic assessment

Daniel Krekel^{a,*}, Remzi Can Samsun^b, Ralf Peters^b, Detlef Stolten^{b,c}

^a Saint-Gobain Sekurit Deutschland GmbH & Co. KG, Herzogenrath Research and Development Center, 52134 Herzogenrath, Germany

^b Forschungszentrum Jülich GmbH, IEK-3: Institute of Electrochemical Process Engineering, 52425 Jülich, Germany

^c Chair for Fuel Cells, RWTH Aachen University, 52072 Aachen, Germany

HIGHLIGHTS

- Amines/imines are most promising adsorbing agents to separate CO₂ from ambient air.
- Energy demand results in 3.65 GJ/t_{CO2} and a second law efficiency of up to 11.83%
- Costs of avoiding CO₂ emissions range from \$ 824 (wind)-1333/t_{CO2} (natural gas)
- CO₂ separation from air is unable to economically compete with CCS.
- Separation from air will not play a vital role in the abatement of the CO₂ problem.

ARTICLE INFO

Keywords:

CO₂ separation from the atmosphere
Techno-economic analysis
Climate change
Carbon capture and storage
CO₂ abatement costs
Polyethyleneimine adsorption

ABSTRACT

This paper assesses the separation of CO₂ from ambient air from a technical and economic standpoint. Reducing CO₂ emissions and their sequestration from the atmosphere is vital to counteract ongoing climate change. The most promising technological options for CO₂ separation are first identified by reviewing the literature and comparing the most important technical and economic parameters. The results point to amines/imines as adsorbing agents to separate CO₂ from ambient air. A system layout is then designed and a technical analysis conducted by solving mass and energy balances for each component. An economic analysis is then performed by applying a specifically-developed model. The total energy demand of the system discussed here is calculated as 3.65 GJ/t_{CO2}. This high energy demand mainly derives from the system-specific implementation of two compressors that compress air/CO₂ and overcome the pressure losses. The second-law efficiency calculated ranges of 7.52–11.83 %, depending on the option of heat integration. The costs of avoiding CO₂ emissions vary between \$ 824 and 1333/t_{CO2}, depending on the energy source applied. The results of this work present higher values for energy demand and costs compared to other values stated in literature. The reasons for this deviation are often insufficient and overoptimistic assumptions in other literature on the one hand, but also relate to the specific system design investigated in this paper on the other. Further case studies reveal that enormous land requirements and investments would be needed to reduce potential CO₂ quantities in the atmosphere to contemporary levels. A comparison between CO₂ removal from the atmosphere and carbon capture and storage technology for coal power plants shows that this technology is not yet able to economically compete with carbon capture and storage. Furthermore, the impact of CO₂ separation on the production costs of industrial commodities like cement and steel demonstrates that CO₂ removal from the atmosphere is not yet a viable alternative to solving the climate change problem. In the long-term, CO₂ separation from ambient air may still play an important role in the sequestration of CO₂ from diluted and dispersed sources, as the technology has the potential for significant further development and optimization.

1. Introduction

Climate change is an all-encompassing challenge facing humanity. The consequences of climate change include, amongst other things, an increase in mean temperature and sea level, the frequent occurrence of

extreme weather events, changes in biodiversity and oceanic acidification. Climate change is result of the greenhouse effect: short-wavelength solar radiation enters the Earth's atmosphere and is partly reflected by surface. As the temperature of the radiation drops on its journey from the Sun to the Earth, its wavelength increases. The

* Corresponding author.

E-mail address: daniel.krekel@saint-gobain.com (D. Krekel).

Nomenclature*List of abbreviations*

CCS	carbon capture and storage
CCUS	carbon capture, utilization and storage
CNG	compressed natural gas
DNI	direct normal irradiation
LNG	liquid natural gas
MEA	monoethanolamine
PEI	polyethyleneimine
PtG	power-to-gas
PtL	power-to-liquids
PtX	power-to-x

List of symbols

Δ	delta [–]
A	surface [m ²]
A	annuity [\$/a]
B_1, B_2	coefficients to account for additional costs [–]
c_p	specific heat capacity [J/mol/K]
c_A	abatement costs [\$/t _{CO2}]
C_B	utilities costs [\$/a]
c_{PC}	specific production costs [\$/t _{CO2}]
C_{BM}	component costs [\$/a] (for components that are not made of carbon steel for an operating pressure of 1 bar)
C_{BM}^0	component costs [\$/a] (for components that are made of carbon steel for an operating pressure of 1 bar)
C_F	manufacturing costs [\$/a]
C_G	overhead costs [\$/a]
C_H	auxiliaries costs [\$/a]
C_L	laboratory costs [\$/a]
C_M	material costs [\$/a]
C_p	staff manufacture costs [\$/a]
C_p^0	acquisition costs [\$/a]
C_{PC}	production costs [\$/a]
C_R	commodities costs [\$/a]
C_{SV}	taxes and insurances costs [\$/a]
C_{UB}	supervision and bureau staff costs [\$/a]
C_W	maintenance costs [\$/a]
F_{CI}	investment costs [\$/a]
F_M, F_P, F_{BM}	coefficients to account for additional costs [–]
g	specific Gibbs energy [J/mol]
Δh_R	specific enthalpy of reaction [J/mol]
\dot{H}	enthalpy flow [W]
i	interest rate [%]
I_{2001}, I_{2012}	Chemical Engineering Cost Plant Index for 2001 and 2012 [–]
k	heat transmission coefficient [W/m ² /K]
K_1, K_2, K_3	component specific coefficients [–]
m	mass [kg]
\dot{m}	mass flow rate [kg/s]
n	polytropic exponent [–]
\dot{n}	molar flow rate [mol/s]

p	pressure [Pa]
q	thermal work [J/mol]
r	reaction rate [mol/m ³ /s]
R	ideal gas constant ($R = 8.314$ J/mol/K)
t	deduction period [a]
T	temperature [°C or K]
V	volume [m ³]
w	specific work [J/mol]
x	sorbent loading [mmol/g]
X	sorbent working capacity [%]
y_i	concentration of component in the gas phase [–]
z_i	concentration of component in the liquid phase [–]
Z	capacity coefficient [–]
η	efficiency [–]
θ	ratio of heat recovery [–]
τ	abatement factor [–]
ν	stoichiometric coefficient [–]

List of indices

0	standard conditions (1013 hPa, 0 °C)
<i>ads</i>	adsorption
<i>cond</i>	condensation
<i>CO2</i>	carbon dioxide
<i>C2H4</i>	ethylene
<i>des</i>	desorption
<i>el</i>	electric
<i>em</i>	emitted
<i>evap</i>	evaporation
<i>F</i>	fluid
<i>g</i>	gas phase
<i>H2O</i>	water/water vapor
<i>HE</i>	heat exchange
<i>i</i>	component i
<i>in</i>	inlet
<i>j</i>	variable j
<i>k</i>	count variable k
<i>l</i>	liquid phase
<i>min</i>	minimal
<i>NG</i>	natural gas
<i>out</i>	outlet
<i>poly</i>	polytropic
<i>product</i>	product
<i>PEI</i>	polyethyleneimine
<i>rev</i>	reversible
<i>s</i>	saturation
<i>sep</i>	separated
<i>sorbent</i>	sorbent
<i>system</i>	system
<i>t</i>	technical
<i>th</i>	thermal
<i>waste</i>	wasted
<i>W</i>	wall

infrared radiation reflected from the Earth's surface cannot completely pass through the "climate gas layer" in the troposphere, and so is reflected back to the Earth [1,2]. Therefore, the terrestrial temperature increases. The "climate gas layer" consists of water vapor as well as CO₂, methane and nitrous oxide etc. Alongside natural emissions of these climate gases, anthropogenic emissions have led to increased amounts of these gases in the troposphere, which are the highest in at least the last 800000 years [3]. Current measurements show

approximately 1800 ppb of methane, 320 ppb of nitrous oxide and 407 ppm of CO₂ [3,4]. Although CO₂ has a global warming potential that is about 1/21 that of methane and about 1/310 that of nitrous oxide over 100 years [5], CO₂, with a current anthropogenic emission of about 38 Gt/a [3], is responsible for about 60% of anthropogenic climate change [6]. As forecast in Pham et al. [6], a CO₂ concentration of 570 ppm can be expected by 2100 as a result of population growth and improving economic conditions. As approximately 1000 ppm could be

hygienically harmful to mankind (according to the United States Environmental Protection Agency (EPA), as noted in Goeppert et al. [7]), a “deadline” will be set for 2300, assuming a conservative increase of CO₂ concentration of 2 ppm/a.

In general, there are three possible means of reducing the amount of CO₂ in the ambient air. Firstly, emissions can be reduced by increasing the efficiency of combustion processes, as in fossil fuel-based power plants or motor vehicles with internal combustion engines. Further options include lowering the energy demand of electrical devices or the restoration of buildings to reduce their demand for heating or air conditioning. Large investment is associated with these measures. Secondly, carbon-based processes could be substituted by, e.g., renewable energy, the use of electric vehicles (based on renewable energy) or low-carbon fuels like compressed natural gas (CNG) or liquid natural gas (LNG) could be expanded. This would reduce emissions but yield higher energy and fuel costs. The third option is to separate CO₂ emissions from the atmosphere and use them as a feedstock for CO₂-based synthesis, such as power-to-gas (PtG, e.g., methanation) and power-to-liquids (PtL, e.g., methanol or urea) or in the beverage industry, greenhouses or to refrigerate food. CO₂ can be separated from the atmosphere using plants’ natural photosynthesis mechanism. The drawbacks of this include low efficiency (0.5–8%), necessitating huge land use and CO₂ emissions during planting, fertilizing and harvesting [7]. Carbon capture and storage (CCS) technologies to separate CO₂ directly at the point of emission, applying absorption or adsorption processes, membranes or cryogenic separation of air, are currently being developed and tested. This technology is applicable for big point emitters like coal power plants, cement plants or steel manufacturing facilities.

As is shown in Fig. 1, up to approximately 60% of global CO₂ emissions could be captured if CCS technology was applied extensively in the industrial, electricity and heat sectors. In other sectors, namely transportation, buildings, services and others, the application of CCS technology is questionable, because of the numerous emitters, all of which would need to be equipped with a CO₂ capturing device (with a corresponding infrastructure, increased weight for aircraft and additional costs, etc.).

In contrast, the direct capture of CO₂ from ambient air offers the advantage of directly capturing one hundred percent of the CO₂ emissions that are “stored in the air”. Stationary, as well as mobile emitters

are covered by this technology. Further advantages are that CO₂ can also be separated after it has been emitted. In other words, emissions from years past that are still stored within the air can be captured at a later point in time. This is not possible with CCS technology. Additionally, ambient air CO₂ capture plants can be directly located next to possible storage sites (e.g., aquifers, depleted coal beds and depleted gas reservoirs). Therefore, no CO₂ infrastructure is necessary, counteracting the need for pipelines or shipment by truck, ship or train and reducing the costs and accompanying CO₂ emissions. Furthermore, numerous CO₂ capture plants could be placed in remote locations like deserts.

Consequently, land availability would not play a role and these plants could potentially be connected to abundant renewable energy sources. Moreover, the agglomeration of a large number of CO₂ capture plants in direct proximity will not only cause a sharp local decrease in CO₂ concentration, but a worldwide decrease, as the air mixture throughout the world is fairly efficient [7]. One argument against direct CO₂ capture from ambient air is that this technology may encourage a “business as usual” mentality (particularly in the energy and transportation sectors), because it is possible to “clean up afterwards”. However, this still does not change the fact that fossil fuels are being depleted and civilization must transition to some kind of renewable energy. Another aspect that must be kept in mind is that this technology, depending on the energy source used to run the system, needs not always be “carbon negative”. There is the possibility that the capture plant emits more CO₂ than is captured during the separation process.

Field and Mach [8] consider direct air capture to be energy-intensive and expensive, yet they state that this technology may eventually provide a useful option for CO₂ removal at scale. They point out the speculative nature of cost, performance and scalability estimates due to the technology’s present immaturity. According to the assessment of Senftle and Carter [9], although this technology may play a role in reaching CO₂ reduction targets in the long term, it will not be sufficient to entirely offset point source emissions in the near term. Wilcox et al. [10] analyze cases where the separation of CO₂ from the air to low and moderate purities can be energetically equivalent to the work required for flue gas separation. They found that enhanced oil recovery and microalgae cultivation are the most beneficial near term applications for the utilization of CO₂ capture from ambient air. Patel et al.

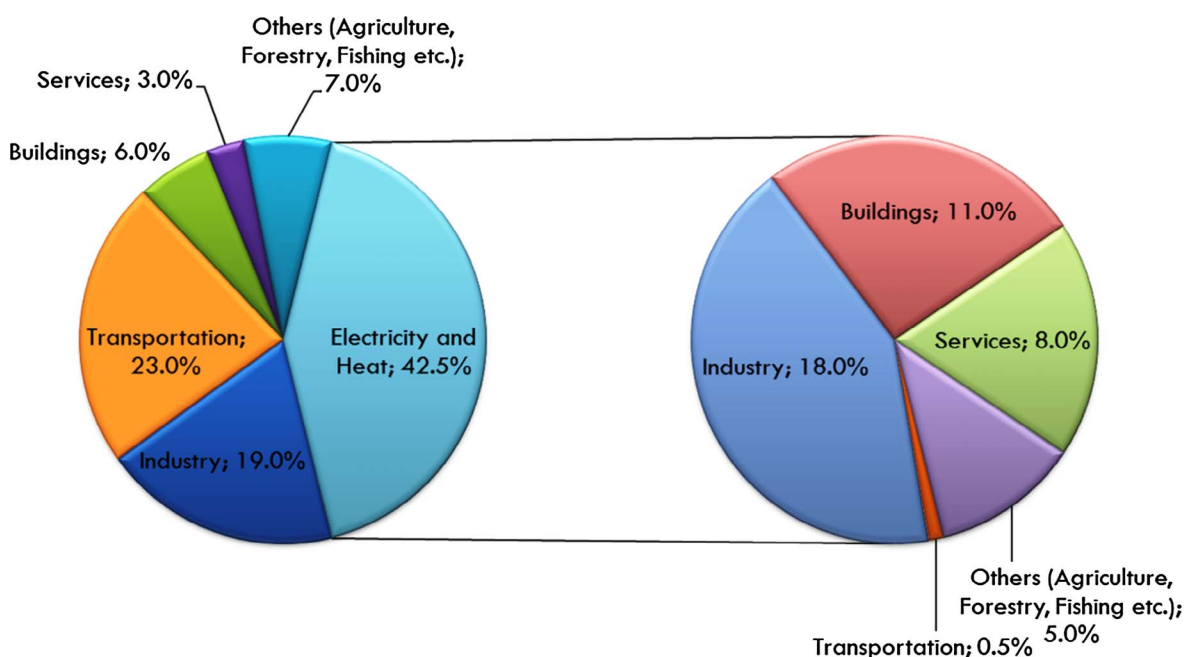


Fig. 1. Global sectoral CO₂ emissions (2013), taken from [92].

[11] refer to direct air capture as the most difficult of all forms of capture and point out the necessity of further research efforts, as this will further enhance the techniques to mitigate CO₂ emissions while reducing their costs. Zhang et al. [12] investigated the environmental performance of power-to-gas process and considered the utilization of waste heat from electrolysis and methanation for their route based on direct air capture. Parra et al. [13] applied both techno-economic and life-cycle assessments to determine the key performance indicators for power-to-gas systems, including direct CO₂ capture from the air.

The most significant aspects, which are highly debated in the literature, include the amount of energy needed to process huge air volume flows to capture considerable amounts of CO₂, as well as the related costs to capture or avoid CO₂ emissions.

With respect to energy demand for direct CO₂ capture from ambient air, it is advisable to consider thermodynamic factors before conducting detailed system calculations. The Gibbs free energy needed (minimum energy demand) to separate, for example CO₂ from a diluted gas mixture can be calculated using Eq. (1) [14]:

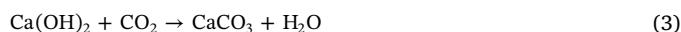
$$\Delta g = R \cdot T \cdot \ln\left(\frac{p^0}{p}\right) \quad (1)$$

This equation, derived from the mass action law, includes the ideal gas constant $R = 8.314 \text{ J}/(\text{mol} \cdot \text{K})$, the temperature T at which the separation process takes place, and the natural logarithm of the quotient of the reference pressure $p^0 = 1013 \text{ hPa}$ and partial pressure of the CO₂ p . With the assumption that CO₂ is separated from the gas stream in ambient conditions ($T = 293 \text{ K}$, $p^0 = 1013 \text{ hPa}$), the needed Gibbs free energy is shown in Fig. 2. The trend of the Gibbs free energy in relation to the partial pressure of the CO₂ reveals an initial exponential decline of the needed Gibbs free energy with increasing CO₂ concentration in the diluted gas stream. Therefore, the minimum energy needed to extract approximately 400 ppm of CO₂ from ambient air aggregates to 19.09 kJ/mol_{CO₂}. This value is in agreement with Schiebahn et al. [14], Socolow et al. [15] and House et al. [16], who estimated minimum energies of between 20 and 21.9 kJ/mol_{CO₂} for similar conditions. With an increasing partial pressure of CO₂, the needed Gibbs free energy decreases linearly. Therefore, the separation of CO₂ from a flue gas stream, which usually contains 10–15% CO₂ (e.g., for post-combustion capture in a coal power plant) only consumes 4.65–5.64 kJ/mol_{CO₂}. It is interesting to note that the separation of CO₂ from air only consumes about four times as much energy that is needed to extract CO₂ from a flue gas stream in a post-combustion capture system in terms of thermodynamics, although the concentration differs by a factor of about ≥ 250 . Additionally, it must be admitted that this calculation is only valid for the complete capture of CO₂ from ambient air and flue gas. For comparison, the correction for less than complete separation is fairly small and corresponds to a fractional reduction of 8% in energy demand, starting with 400 ppm CO₂ and 22%, starting with 12% CO₂ if the fraction of captured CO₂ is only 0.5 [15]. Thus, with respect to CO₂ separation from ambient air as stated above, a literature review was conducted to identify the most promising capture technology for this process. Then, a system layout for the identified separation process was designed so that a technical system assessment could be performed. A detailed economic analysis for the selected system design complemented the technical analysis in order to enable a complete assessment of the technology. Furthermore, the techno-economic assessment was extended with different case studies to consider the sensitivity of the assumed parameters and estimate the future global role of the investigated technology and its possible impact for emission reduction targets. On the basis of the findings, the CO₂ capture from ambient air is compared to the competing carbon capture and storage technology. Finally, the influence of this technology on the production costs of exemplary sectors with high emissions was evaluated. The results of this contribution help to illuminate the advantages and hurdles associated with the separation of CO₂ from ambient air and allow a realistic

judgement of its potentials.

2. Literature analysis

Numerous technologies and materials for capturing CO₂ from ambient air are discussed in the literature, such as absorption/adsorption processes with inorganic chemisorbents, amines/imines, zeolites or anionic exchange resins, to name just a few. Processes applied for carbon capture and storage cannot be directly transferred to CO₂ separation from the air due to the humidity of the air, very low CO₂ concentrations and the necessity to process close to ambient temperature and pressure conditions [7]. The purpose of this paper is not to review the literature in detail, because this has already been conducted by others, for example Goeppert et al. [7]. Koytsoumpa et al. [17] report that adsorption technology for CO₂ capture receives ever more attention due to its lower energy consumption in their review paper. Technologies that have been intensively investigated are the adsorption of CO₂ on amines/imines [7,18–36]; and the absorption on inorganic chemisorbents like CaO, Ca(OH)₂ [7,37–41], 2NaOH [15,16,42–46] or K₂CO₃ [47–49]. Amines are derivatives of ammonia, which are immobilized on solid supports like silica, polymers, porous materials, metals or carbon fibers, inter alia. These are classified into three classes, depending on their support and bonding to it. During the capture process, CO₂ is adsorbed on the amine/imine at temperatures of about 10–75 °C and ambient pressure, and subsequently desorbed at temperatures of approximately 50–130 °C. The literature lists advantages like operation close to ambient conditions, as well as cheap and easy production. Disadvantages include the early development status and that long-term stability has yet to be clarified. Degradation of the amines/imines or support could occur due to oxidation reactions at high operating temperatures or the blockage of active centers by NO_x or SO_x [7]. Adsorption processes with CaO, Ca(OH)₂, 2NaOH or K₂CO₃ all have in common that CO₂ reacts with the basic material to form carbonates, as shown in the following Eqs. (2)–(5):



The processes differ from each other in terms of applied materials, reaction kinetics and reaction parameters (temperature, pressure) and solubility of the reaction species in water, as well as system design. For convenience, this is not discussed here, but can be checked in the cited literature [7,18–36]. The general advantages of the CaO, Ca(OH)₂ and 2NaOH processes are that these are standard operations known from the cement industry and the charge materials are inexpensive, non-toxic and adequately available. However, all of the absorption processes listed above comprise reaction steps to retrieve the basic material and

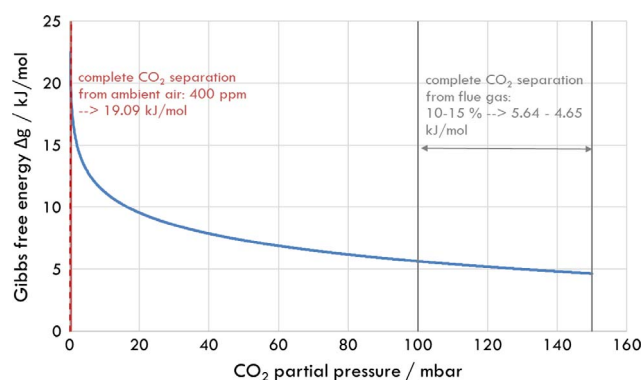


Fig. 2. Necessary Gibbs free energy to separate CO₂ from a diluted gas stream.

separate the CO_2 for subsequent storage, which are very energy-intensive. The regeneration, also called calcination, runs at temperatures from about 800–1200 °C for the CaO and $\text{Ca}(\text{OH})_2$ cycles [7,37–41] and at 900 °C for the 2NaOH cycle [15,16,42–46]. In contrast, the K_2CO_3 cycle only requires regeneration temperatures of 150–350 °C [47–49]. As for the amines/imines, long-term stability is not yet known for all of the adsorption processes discussed here.

To identify which of the investigated processes has the highest potential for application in a CO_2 separation process from ambient air, data for significant process parameters were collected from 35 sources [7,15,16,18–49] and compared to each other. The results are shown in Fig. 3. The parameters selected for comparison were cyclability, the consumption of electrical and thermal work, possible loading of CO_2 on the sorbent and operating costs. For parameters indicated by green, high values are advantageous; for those indicated by red, they are disadvantageous. Due to a lack of information in the literature, it was not possible to collect data for each process and parameter. As there are discrepancies in the literature (depending on the system design and assumptions, etc.), optimal and worst (min) values are indicated in Fig. 3. It is obvious that the $\text{Ca}(\text{OH})_2$ process (the CaO process was neglected due to limitations in reaction kinetics compared to the $\text{Ca}(\text{OH})_2$ process), as well as the 2NaOH process, have significant drawbacks in terms of demand for electrical and thermal work. For the $\text{Ca}(\text{OH})_2$ process, thermal work ranges from 207 to 45000 $\text{kJ}_{\text{th}}/\text{mol}_{\text{CO}_2}$ in the literature, while for the 2NaOH process, the demand for thermal work ranges from 225 to 648 $\text{kJ}_{\text{th}}/\text{mol}_{\text{CO}_2}$ and for electrical work from 31 to 121 $\text{kJ}_{\text{el}}/\text{mol}_{\text{CO}_2}$ [7,15,16,18–49]. With respect to these values, high costs can be anticipated, which are calculated to be around \$ 10–1700/ t_{CO_2} for the $\text{Ca}(\text{OH})_2$ cycle and \$ 49–600/ t_{CO_2} for the 2NaOH cycle. As both processes have no clear advantage in terms of cyclability and loading, they are excluded from further investigation. If the remaining amine/imine cycle is compared to the K_2CO_3 process, it becomes clear that none of these processes have clear advantages over the other when thermal and electrical work are considered. Furthermore, cyclability is comparable, although a certain advantage is visible for the K_2CO_3 process. Nevertheless, it should be remembered that thousands

of cycles must be performed before the long-term stability can be properly judged. In terms of costs, the K_2CO_3 process may be cheaper, as \$ 20/ t_{CO_2} is stated in the literature, whereas \$ 30–425/ t_{CO_2} are quoted for the amine/imine cycle. One very important parameter, namely the loading of CO_2 on the sorbent, points to amines/imines as the most promising process for CO_2 separation from ambient air. Values ranging from 0.11 to 3.34 $\text{mmol}_{\text{CO}_2}/\text{g}_{\text{sorbent}}$ are reported for amines/imines. For the K_2CO_3 cycle, the loading of 0.23–1.11 $\text{mmol}_{\text{CO}_2}/\text{g}_{\text{sorbent}}$ is possible. The higher this parameter is, the cheaper the process can be, as the material costs decrease. The demand for thermal and electrical work may also decrease, as less material must be processed. Additionally, the system might be designed to be smaller. These advantages in relation to the loading of CO_2 on the sorbent makes amines/imines the most promising technology for the separation of CO_2 from ambient air. As a result, a system layout was designed with an adsorber/desorber unit, which is equipped with an imine to separate the CO_2 . The system design and methodology of the technical and economic system analysis are described in the following section.

3. Methodology

This section describes the system design and the methodology applied for the technical and economic analysis.

3.1. System design

The system's design is shown in Fig. 4. Ambient air is sucked into the system by compressor 1, which overcomes the pressure losses within the system. Afterwards, the air comes into contact with polyethyleneimine (PEI), which is immobilized, e.g., on silica as support in the fluidized bed adsorber. During the exothermal adsorption reaction at approximately 20 °C, CO_2 is adsorbed onto the PEI/support. The cyclone, which is positioned at the adsorber outlet, separates air from the PEI/support and CO_2 . Next, CO_2 is desorbed from the PEI/support in the fluidized bed desorber at 130 °C. Since the separate adsorber and desorber units are implemented into this system, continuous CO_2

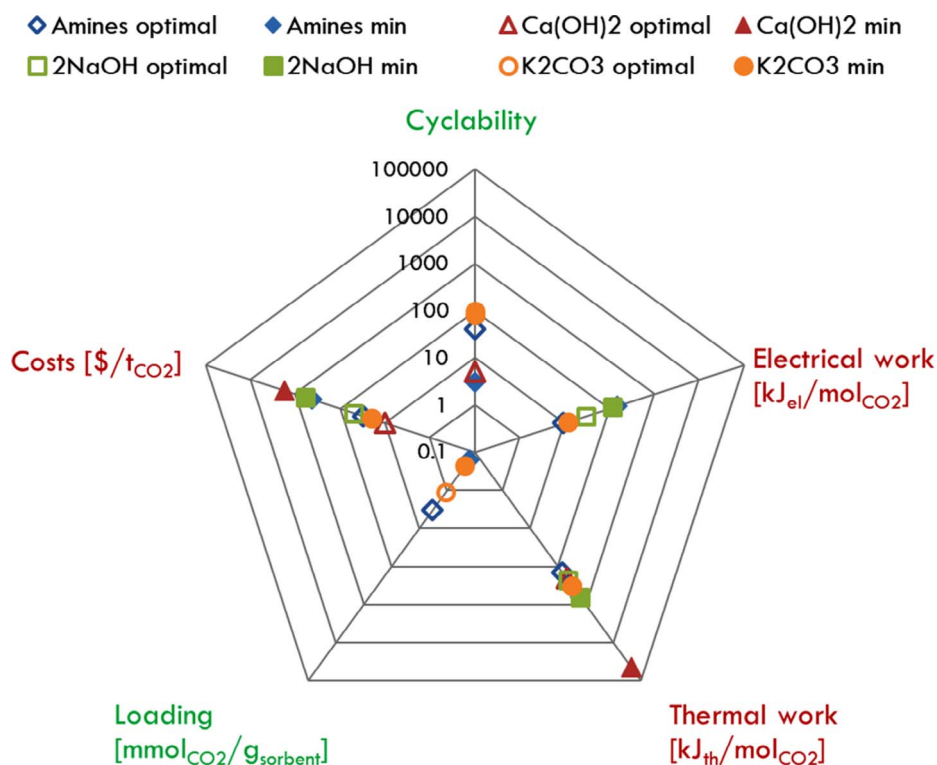


Fig. 3. Comparison of processes for CO_2 separation from air in terms of different process parameters.

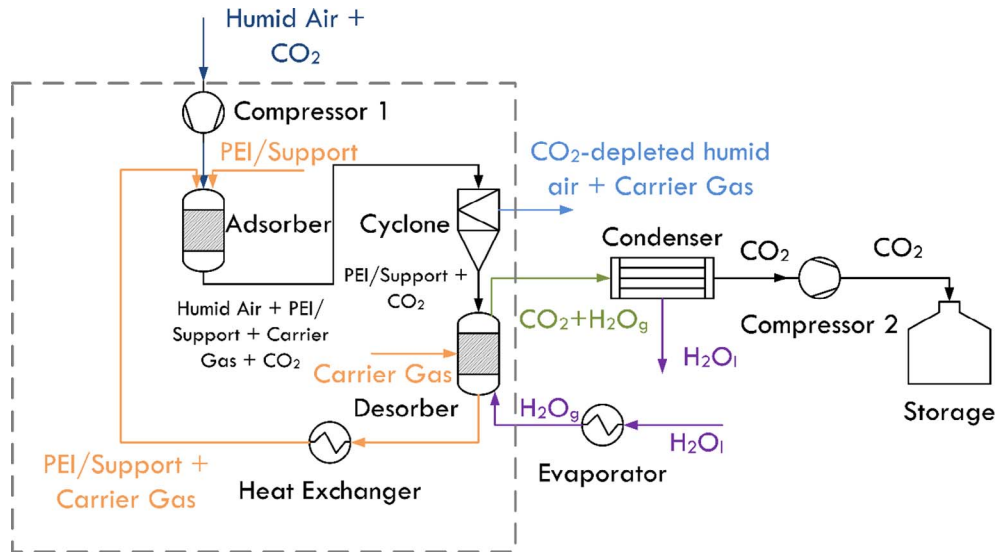


Fig. 4. System flow chart of the analyzed CO₂ separation plant.

separation is possible, without the need for cycling between adsorption and desorption. Water vapor with a mass flow ratio of $\dot{m}_{\text{CO}_2}/\dot{m}_{\text{H}_2\text{O}} = 1$ is added to the desorber as a purging gas and to decrease the thermal degradation of the PEI/support [32]. Behind the desorber, PEI/support is recycled with a carrier gas to the adsorber. Before entering the adsorber again, the heat recovery lowers the PEI/support temperature down to 20 °C. CO₂ and water vapor are transported to the condenser, in which water vapor is almost completely condensed in order to compress CO₂ in a subsequent step to 10 MPa for storage in something such as an aquifer. The separation plant is designed for a capacity of 14150 t_{CO2}/a. The basics of this system were adopted from the system layout described in Zhang et al. [32]. The part of the system design that was adopted from Zhang et al. is indicated by the dashed frame in Fig. 4. This means that only minor changes were made to this part of the system. The other system components were then added to complete the CO₂ separation plant for the detailed technical and economic system analysis conducted in this contribution. Some general assumptions for the system calculation are listed below:

- Humid air (as also applied by Zhang et al. [32]; here 1 mol.% H₂O) enters the system with a CO₂ concentration of 500 ppmv (basic case)
- No sorbent loss was considered
- Ideal gas behavior is assumed for all gases in the system
- $p_{\text{system}} = 1013 \text{ hPa} = \text{const.}$
- A 20% heat loss is assumed for the complete system.

In the next section, the methodology for the technical analysis of each system component, as well as the complete system, is described.

3.2. Technical system analysis

3.2.1. Compressor 1

The work needed to operate compressor 1 and compensate for the pressure losses in the system was taken from Zhang et al. [32] and amounts to 132 kJ_{el}/mol_{CO2}. Therefore, no separate pressure drop calculation was conducted. This value is valid for all case studies presented later in this contribution, as the air volume flow is kept constant in any case.

3.2.2. Adsorber

Air coming from compressor 1 enters the adsorber, as does PEI/support with carrier gas. Mass and energy balances needed to be solved to calculate the molar flows and temperatures resulting from the mixing

and exothermal adsorption reaction within the reactor. The stationary mass and energy balances can be calculated using Eqs. (6) and (7) [50]:

$$0 = \dot{n}_{i,\text{in}} - \dot{n}_{i,\text{out}} + V \cdot \sum_{j=1}^k \nu_{ij} \cdot r_j \quad (6)$$

$$0 = \dot{H}_{\text{in}} - \dot{H}_{\text{out}} + k \cdot A \cdot (T_W - T_F) + V \cdot \sum_{j=1}^k r_j \cdot (-\Delta h_{Rj}) \quad (7)$$

In Eq. (6), all incoming and outgoing molar flows $\dot{n}_{i,\text{in}}$ and $\dot{n}_{i,\text{out}}$ must be subtracted. Furthermore, the change in the amount of substance $V \cdot \sum_{j=1}^k \nu_{ij} \cdot r_j$ (V is the reaction volume, r_j the reaction rate of reaction j and ν_{ij} the stoichiometric coefficient of component within reaction j) caused by the different reactions occurring must be considered. However, this was neglected here for the sake of simplicity. In addition, the molar flow of the carrier gas was also neglected. In Eq. (7), incoming and outgoing enthalpy flows are subtracted. Due to very small molar flows in comparison to the incoming air, the enthalpy flows of PEI/support and carrier gas were neglected. In general, the heat exchange with the reactor wall ($k \cdot A \cdot (T_W - T_F)$) must be taken into account, where k is the heat transmission coefficient, A is the heat transfer surface and $(T_W - T_F)$ the temperature difference between the reactor wall and fluid. This term was disregarded for the adsorber, as an overall heat loss of the complete system of 20% was considered in the cyclone. The term $V \cdot \sum_{j=1}^k r_j \cdot (-\Delta h_{Rj})$ considers the change in enthalpy flow due to the chemical reactions occurring. The reaction enthalpy ($-\Delta h_{Rj}$) of the adsorption reaction was once again adopted from Zhang et al. [32] and is $-90 \text{ kJ/mol}_{\text{CO}_2}$. It was further assumed that the heat of the adsorption reaction does not change in respect to the sorbent loading. According to the highest values reported in the literature [30], a sorbent capacity of $x_{\text{sorbent}} = 3.5 \text{ mmol}_{\text{CO}_2}/\text{g}_{\text{sorbent}}$ and 100% adsorption efficiency (meaning that all of the CO₂ entering the adsorber is adsorbed onto the PEI/support) were assumed. Fluid properties like molar mass, density, enthalpy or heat capacity for the different species handled in the CO₂ separation plant were either calculated by polynomial equations from NIST Database [51] or taken from [51] and Zhang et al. [32]. Additional geometrical and process parameters of the adsorber are listed in the Appendix A (Table 6).

3.2.3. Cyclone

The humid air and the carrier gas are separated from the PEI/support and CO₂ in the cyclone by centrifugal force. As was already stated above, the model described in this contribution assumes a 20% heat loss

within this component. Additional geometrical and process parameters of the cyclone are listed in the [Appendix A \(Table 7\)](#).

3.2.4. Desorber

After the cyclone, PEI/support, CO₂ and water vapor flow into the desorber, where PEI/support is separated from CO₂ and water vapor at 130 °C. The heat needed to drive the endothermal desorption process q_{des} can be calculated with reasonable accuracy using Eq. (8) [32]:

$$q_{des} = \frac{1-\theta}{X_{sorbent}} \cdot c_{p,PEI} \cdot (T_{des} - T_{ads}) - \Delta h_{R,ads} \quad (8)$$

In this equation, θ is the degree of possible heat recovery achieved by implementing heat exchangers in the system. As heat exchangers are calculated separately in the system design described here, the degree of heat recovery in the desorber is zero. The working capacity of the sorbent $X_{sorbent}$ is the loading of the sorbent expressed in percent. The assumed 3.5 mmol_{CO2}/g_{sorbent} (see above) corresponds to a working capacity of 15 wt%. The specific heat capacity $c_{p,PEI} = 3060 \frac{J}{mol \cdot K}$ was adopted from Zhang et al. [32] and $(T_{des} - T_{ads})$ considers the temperature difference between the adsorption and desorption processes. The specific reaction enthalpy of the adsorption process must be subtracted to account for the energy needed to break the bond between CO₂ and the sorbent. Additional geometrical and process parameters of the desorber are listed in the [Appendix A \(Table 8\)](#).

3.2.5. Heat exchanger

Three heat exchangers are used in the CO₂ separation plant, namely the evaporator, condenser and heat exchanger for heat recovery of the recycled PEI/support stream. The heat exchange in the evaporator and the recovery heat exchanger can be calculated by applying the first law of thermodynamics (Eq. (9)):

$$q_{HE} = c_{p,1} \cdot (T_2 - T_1) + \Delta h_{R,evap} + c_{p,2} \cdot (T_3 - T_2) \quad (9)$$

The amount of heat exchanged depends on the specific heat capacity of the fluid that receives or rejects the heat, multiplied by the difference in temperature before and after the heat exchange (sensible heat). For the calculation of the heat exchanger, which recovers the sensible heat of the PEI/support, the first term of Eq. (9) is sufficient. The PEI/support is cooled down from 130 °C (desorption) to 20 °C (adsorption)

without a phase change. As was stated above, the carrier gas is neglected in these calculations. In the case of the evaporator, an amount of demineralized water corresponding to $\dot{m}_{CO2}/\dot{m}_{H2O} = 1$ is heated up from 20 °C (ambient temperature) to 100 °C, evaporates and is then further superheated up to 130 °C (temperature level desorber). Therefore, the latent heat of the phase change of water $\Delta h_{R,evap} = 40.66 \text{ kJ/mol}_{H2O}$ must also be considered. The sensible heat required to heat the water vapor from 100 °C to 130 °C is considered with the specific heat capacity of water vapor in this temperature range.

Before the heat exchange in the condenser can be calculated by the energy balance, a phase equilibrium calculation is first needed. Assuming ideal gas behavior, the binary gas/liquid phase equilibrium between CO₂ and H₂O can be calculated by applying Eqs. (10)–(13) [52,53]:

$$y_{CO2} \cdot p = z_{CO2} \cdot p_{s,CO2} \quad (10)$$

$$y_{H2O} \cdot p = z_{H2O} \cdot p_{s,H2O} \quad (11)$$

$$y_{CO2} + y_{H2O} = 1 \quad (12)$$

$$z_{CO2} + z_{H2O} = 1 \quad (13)$$

In these equations, y_i is the concentration of component in the gas phase and z_i the concentration of component in the liquid phase. The pressure of the phase equilibrium is p and $p_{s,i}$ represents the saturation pressure of component i . If the mixture is cooled down to 20 °C in the condenser, almost all of the water vapor transforms into liquid and the remaining gas phase consists of CO₂ with a molar fraction of $y_{CO2} = 0.977$ and the remaining H₂O. In this design, the condensed water vapor is wasted and not recycled. In addition to the heat released during condensation, the sensible heat during the cooling-down of the mixture to the mixture condensation start temperature of approximately 90 °C also contributes to the overall heat released by this system component. Additional geometrical and process parameters of the heat exchangers are again listed in the [Appendix A \(Tables 9–11\)](#).

3.2.6. Compressor 2

The necessary electrical work to compress the CO₂ to 10 MPa for storage is calculated by assuming polytropic compression. The specific reversible technical work for polytropic compression can be calculated using Eq. (14) [54]:

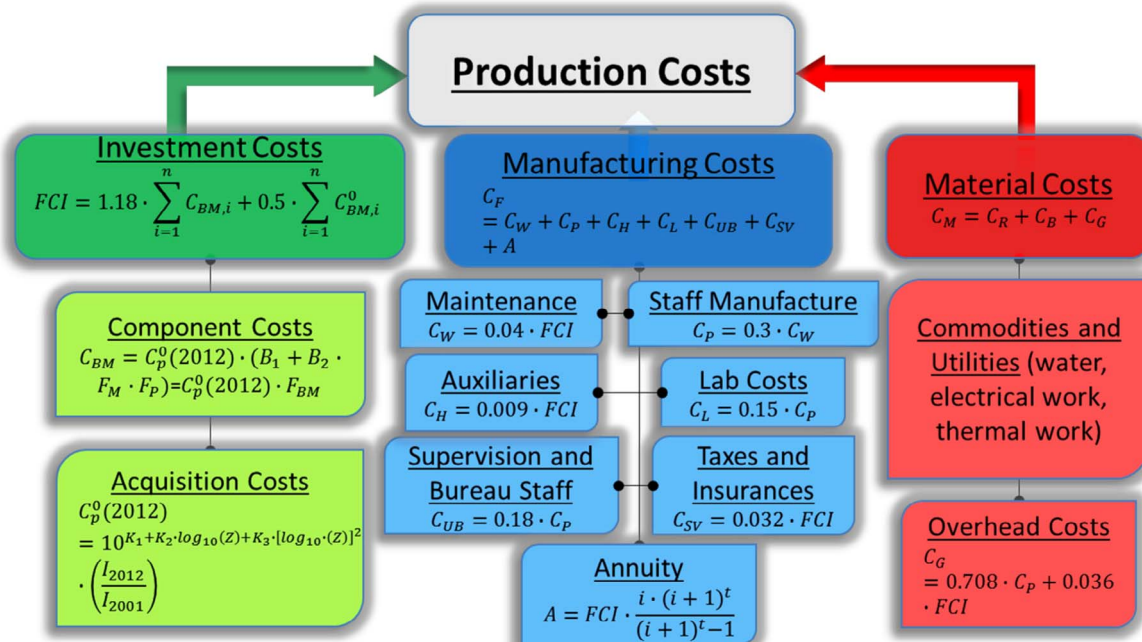


Fig. 5. Model for the economic analysis of the CO₂ separation plant, taken from [15,34,56].

$$w_{t,poly,rev} = \frac{n \cdot R \cdot T_1}{n-1} \cdot \left[\left(\frac{p_2}{p_1} \right)^{\frac{n-1}{n}} - 1 \right] \quad (14)$$

In this equation, n is the polytropic exponent, which was assumed to be 1.3, R is the ideal gas constant, T_1 is the fluid temperature before compression and p_1 and p_2 are the pressures of the fluid before and after compression, respectively. To determine the technical work, the polytropic efficiency must be considered and in this case was assumed to be 0.7. For the subsequent calculation of the overall electrical work needed to compress CO₂ to 10 MPa, the mechanical efficiency of the electric motor, which powers the compressor, must also be considered. In this contribution, a mechanical efficiency of 0.9 was chosen. The CO₂ changes to the subcritical state due to compression and can be stored in this state [55].

3.3. Economic system analysis

For the economic analysis, a model was developed that is mainly based on the explanations of Otto [56] and supplemented with information from Socolow et al. [15] and Kulkarni et al. [34]. The structure of the economic model is shown in Fig. 5. The production costs, i.e., the costs for capturing a ton of CO₂ with the ambient air separation plant described in this contribution, comprise the investment costs, manufacturing and material costs. The investment costs FCI include the acquisition costs C_p^0 and component costs C_{BM} . The acquisition costs are those for the specific components of the CO₂ separation system. The variables K_1 , K_2 , K_3 are component-specific coefficients. The capacity coefficient Z accounts for the power of a compressor, the surface of a heat exchanger or the volume of a reactor. All of these coefficients are listed in the Appendix A (Table 12) and are valid for the year 2001 ($I_{2001} = 394$) [56]. To generate more ongoing data, the Chemical Engineering Cost Plant Index I is considered for 2012 ($I_{2012} = 584.6$) [56]. In terms of simplicity, the cyclone was calculated as a vertical vessel. In addition to the acquisition costs, the component costs also incorporate the costs of the installation material, salaries, transportation, insurance, taxes, costs for planning and the dimensioning of components, as well as overhead costs with the factors B_1 , B_2 , F_M , F_P and F_{BM} . These coefficients are also listed in the Appendix A (Table 13). The costs of each component are added up to calculate the total investment costs. Additionally, an 18% surcharge for unplanned costs is added to the component costs in modified condition (i.e., costs for components that are not made of carbon steel for an operating pressure of 1 bar). 50% of the component costs in the basic condition (i.e., components that are made of carbon steel for an operating

pressure of 1 bar) are added to the investment costs to account for the costs for additional facilities, improvement of land and the storage of educts and products. In this calculation, all components are assumed to be constructed of carbon steel for an operating pressure of 1 bar, and so there is no difference between the basic component condition and modified condition.

The manufacturing costs C_F include the costs for maintenance C_W , staff (manufacture C_P , supervision and bureau C_{UB}), auxiliaries C_H , laboratory C_L , taxes and insurance C_{SV} , which accumulate in the course of the operation of the CO₂ separation plant. The equations shown in Fig. 5 are used to calculate the different cost centers. The investment costs are incorporated into the manufacturing costs by the annuity. Annuity A reflects the repayment and interest that need to be paid on the bank loan. A payback period of $t = 20$ a was assumed at an interest rate of $i = 7.2\%$. For the subsequent calculations, it was assumed that CO₂ separation plants will be unserviceable after 20 years of usage and that they will be replaced by new ones. Furthermore, future changes in the costs of a CO₂ separation plant were not considered.

The material costs C_M include the costs of commodities C_R (water, natural gas, etc.) and utilities C_B (thermal work, electrical work), as well as the overhead costs C_G . In this analysis, the costs for the demineralization of the water (purging gas) are not considered. Overhead costs include costs for transportation, storage and packaging, amongst others. These costs are calculated based on the assumption that the CO₂ separation plant operates 6000 h of full load hours per year.

Investment, manufacturing and material costs were regarded as static, which means that no changes in prices were considered for future calculations. This assumption was made due to the uncertainty associated with the development of the manufacturing costs and different prices for commodities and utilities. In contrast to the constant investment, manufacturing and material costs, it was generally assumed that CO₂ separation plants will be able to separate CO₂ from ambient air more efficiently in future (independent of the CO₂ concentration in the atmosphere), which leads to a reduction in the specific costs of separating one ton of CO₂.

4. Results

4.1. Technical system analysis

For the technical system analysis, the methodology described in Section 3.2 was applied to identify all thermal and electrical sources and sinks. An overview of the system with all sources and sinks and the amount of rejected and necessary thermal and electrical work is shown in Fig. 6. With respect to the thermal work, heat sources were the

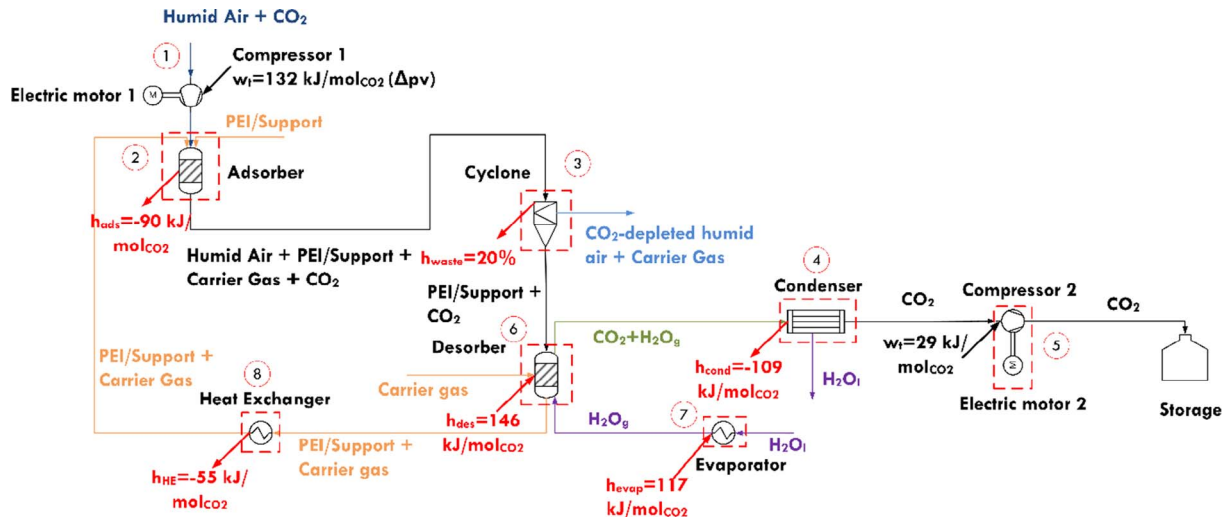


Fig. 6. Detailed system flow chart of the analyzed CO₂ separation plant, including thermal and electrical sources and sinks.

condenser, adsorber and heat exchanger (in order of decreasing rejected heat). The thermal work amounts to $-254 \text{ kJ/mol}_{\text{CO}_2}$ separated. Heat sinks were the desorber, evaporator (in the order of decreasing necessary heat) and wasted heat, which was assumed to occur in the cyclone. The heat sinks amount to $263 \text{ kJ/mol}_{\text{CO}_2}$. As the amount of rejected and necessary heat are comparable, it was assumed that sources and sinks can be balanced with an appropriate heat management regime. Therefore, full heat integration was a basic assumption for all subsequent case study calculations. However, although the number of heat sources and sinks are comparable, hot and cold streams cannot be connected arbitrarily due to the varying temperature levels of the different streams. The suitability of full heat recovery can be checked by means of a pinch point analysis [57]. A pinch analysis with a pinch of 4 K showed that for the system proposed in this paper, $101 \text{ kJ/mol}_{\text{CO}_2}$ of heat needs to be supplied, while $255 \text{ kJ/mol}_{\text{CO}_2}$ of cooling is necessary to close the thermal balance. Although this fact was neglected in subsequent calculations, it must be noted that the CO_2 separation system in this paper was designed conservatively with respect to the heat sinks. For example, it is not necessary to use a mass flow ratio of $\dot{m}_{\text{CO}_2}/\dot{m}_{\text{H}_2\text{O}} = 1$ as a purging gas for the desorber. As a counter example, Zhang et al. only used a water vapor quantity corresponding to 25% of the CO_2 quantity to flush the desorber [32]. Therefore, our proposed system design has the potential for improved heat management, so that the assumption of full heat integration is more realistic.

With reference to the mandatory electrical work, compressors 1 and 2 add up to $161 \text{ kJ/mol}_{\text{CO}_2}$. It is obvious that compressor 1, which circulates large amounts of air through the system and overcomes the pressure losses, accounts for approximately 82% of the electrical work needed. Therefore, a future target must be to develop a system with the lowest possible pressure drop in order to decrease the amount of electrical work needed.

To determine the efficiency of the system, the defined efficiency factor (“second-law efficiency”) from House et al. [16] was used for the proposed system here. This efficiency factor, shown in Eq. (15), relates the thermodynamic minimum Gibbs energy (calculated from Eq. (1)) needed to separate CO_2 from a diluted gas stream to the Gibbs energy of the thermal and electrical work applied in the designed CO_2 separation plant.

$$\eta = \frac{\Delta g_{\min}}{\Delta g_{\text{th}} + \Delta g_{\text{el}}} \quad (15)$$

Table 1
Results of the economic system analysis.

Investment costs								
Compoent	Adsorber	Desorber	Evaporator	Heat exchanger	Condenser	Cyclone	Compressor 1/2	E-motor 1/2
C_P^0 [10 ⁶ \$]	1.89	0.07	0.24	0.03	0.27	3.04	0.67/0.21	0.2/0.12
C_{BM} [10 ⁶ \$]	7.57	0.26	0.7	0.09	0.79	12.39	2.55/0.81	0.3/0.18
FCI [10 ⁶ \$]	43.08							
Manufacturing costs								
Cost Center	C_W	C_P	C_{UB}	C_H	C_L	C_{SV}	A	C_F
[10 ⁶ \$/a]	1.72	0.52	0.09	0.39	0.08	1.38	4.13	8.31
Material costs								
Cost Center	Water		Electrical work (natural gas)		Overhead costs		C_M	
[10 ⁶ \$/a]	0.04		0.95		1.92		2.91	
Production costs								
C_{PC} [10 ⁶ \$/a]	11.21				Specific production costs (separation costs) [\$/t _{CO2}]		792 (@14150 t _{CO2} /a)	

On the one hand, if full heat integration is considered, the system efficiency is 11.83% for a CO_2 concentration of 500 ppmv in the atmosphere. On the other, if no heat integration is possible (all required heat must be supplied from external sources), the efficiency is only 7.52%. In comparison to both efficiency values calculated here, House et al. [16] state that second-law efficiencies of CO_2 separation processes from ambient air will likely be significantly below 10%. They also calculated second-law efficiencies of 2.4–50% based on data provided in other publications [16]. The efficiencies calculated for the presented CO_2 separation plant are therefore comparable to the values stated in the literature. The fairly high value of 50% is derived from the work of Lackner [33], where the design was based on the laboratory results of a strong-base ion-exchange resin. Lackner assumed that the condensation of water and heat from compression are sufficient to cover the heat demand. Unfortunately, the air energy consumption for the mechanical operation of the air collector was estimated to be rather small [33], which resulted in the very high second law efficiency described by House et al. [16]. In this work, it was shown that the air compression has a much higher electricity demand of $132 \text{ kJ}_{\text{el}}/\text{mol}_{\text{CO}_2}$, which corresponds to $3 \text{ GJ}_{\text{el}}/\text{t}_{\text{CO}_2}$, according to the data given by Zhang et al. [32]. This is due to the utilization of a cyclone in the process scheme. Broehm et al. [58] published a techno-economic review indicating that most of the proposed direct air capture systems demand between 0.36 and $0.44 \text{ GJ}_{\text{el}}/\text{t}_{\text{CO}_2}$. Both groups stated that later systems will require a higher share of thermal energy [32,58]. Finally, Broehm et al. [58] conclude a total energy demand of about $10 \text{ GJ}/\text{t}_{\text{CO}_2}$ for direct air capture systems. This work results in a total energy demand of nearly $6 \text{ GJ}/\text{t}_{\text{CO}_2}$ for thermal and electrical energy if the results of the pinch analysis are considered, and $9.65 \text{ GJ}/\text{t}_{\text{CO}_2}$ in the case that no heat integration is implemented.

4.2. Economic system analysis

The economic model described in Section 3.3 was applied to estimate the costs of the CO_2 separation process. The results for the investment costs of each system component, manufacturing costs and material costs, which constitute the production costs, are listed in Table 1. The cyclone has the highest acquisition and component costs due to its large volume. Thereafter, the adsorber contributes to the investment costs with \$ 7.57 million dollars component costs. The costs of compressor 1 are also noticeable, accounting for \$ 2.55 million of the

component costs. For the remaining system components, component costs vary between \$ 0.18–0.81 million. The total investment costs are \$ 43.08 million for the CO₂ separation plant with a capacity of 14150 t_{CO2}/a. The costs for the sorbent PEI/support are not considered in this calculation. In their techno-economic review, Broehm et al. published specific values of between \$ 300 million and \$ 3000 million/Mt_{CO2} [58], the upper limit corresponding to the result of the detailed analysis presented here. The high investment is compelled by the cyclone, with a share of nearly 29% of the investment costs, i.e., \$ 870 million/Mt_{CO2}.

The biggest contribution to the manufacturing costs of nearly 50% is the annuity due to the high investment costs. After the annuity, maintenance, taxes and insurance significantly impact the manufacturing costs. The sum of all the cost centers listed in Table 1 equals \$ 8.31 million per year.

The material costs add up to \$ 2.91 million per year. The overhead costs account for the biggest segment of these, at \$ 1.92 million per year. The costs for the educt water only account for \$ 0.04 million per year, although no recirculation of the water was considered (water from the condenser could be recycled to the evaporator). The educt costs of water were assumed to be \$ 3/m³. Additional costs to demineralize the water were neglected here. Considering demineralization costs of \$ 1.321/m³ [59], the costs to capture/avoid CO₂ emissions would increase by 0.13–0.17 %, depending on the energy source. Furthermore, as described in this section above and in the global system assumptions in Section 3.1, no costs for the PEI/support and its replacement were considered. It is noteworthy that the costs to separate/avoid CO₂ emissions would increase by 2.0–2.6 % (depending on the energy source) if the total amount of the PEI/support in the adsorber and desorber (total sum: 8000 kg) needs to be replaced after 1000 cycles (assumed price for PEI/support: \$ 3/kg based on a PEI price from [60]). In the literature, PEI material was tested for up to 80 cycles [23]. In comparison to PEI which is a new and promising technology for CO₂ separation, standard monoethanolamine (MEA) technologies are well known in chemical industry. For CO₂ separation from flue gas of lignite power plants MEA materials are tested up to 3700 h [61–64]. MEA solutions were exchanged due to solvent degradation afterwards. New sorbent materials were tested for 55000 h without strong degradation effects [65]. Here we assumed a higher value of 1000 cycles for PEI in comparison to the demonstrated value in literature considering its further development in the future. Furthermore, it must be noted that the assumed value is conservative compared to other technologies like

MEA. As full heat integration within the system was expected (see above), there is no cost center for heating in Table 1. If the electrical work needed by the compressors is supplied by the combustion of natural gas in a combined cycle power plant process (\$ 0.0661/kWh_{el} [34]), for example, the costs would amount to \$ 0.95 million per year.

Assuming the above-mentioned values, the production costs total \$ 11.21 million per year. If the amount of captured CO₂ is considered (14150 t_{CO2}/a), the specific production costs, i.e., the costs for CO₂ separation, total \$ 792/t_{CO2}.

As is outlined in Section 3.3, future changes in the costs of a CO₂ separation plant were not considered. If this technology was widely utilized, the price would be expected to drop in accordance with the learning curve. Due to the high share of the investment costs in the production costs calculation, in order to consider this development from an abstract perspective, a further case was calculated assuming an exemplary cost reduction of 25% of the investment costs for the CO₂ separation plant. In this case, the costs for CO₂ separation amount to \$ 612/t_{CO2}.

In addition, some simplifying assumptions were made during the system analysis, such as neglecting water demineralization or the costs for the acquisition and replacement of the PEI/support (see above). Incorporating the aforementioned points would increase the overall costs for CO₂ separation from ambient air by approximately 2.1–2.7%, depending on the energy source.

In addition to the basic case calculated (atmospheric CO₂ concentration: 500 ppmv), a sensitivity analysis will be conducted in the following section to evaluate the effect of an increasing CO₂ concentration and different energy sources powering the separation process on the energy demand and process costs.

4.3. Case study 0: system sensitivity analysis

The sensitivity analysis evaluates the impact of a prospective increase in CO₂ concentration on the energy demand and the costs of the separation process. The results of this analysis are shown in Fig. 7, which indicates the necessary work/power and costs needed to operate the separation process dependent on the atmospheric CO₂ concentration. As full heat integration is assumed, thermal work/power is equal to zero, independent of the CO₂ concentration. The electrical work is shown as a specific value in GJ_{el}/t_{CO2} and is therefore also independent of the CO₂ concentration. The necessary electrical work is calculated as 3.65 GJ_{el}/t_{CO2}, which corresponds to the above-mentioned 161 kJ_{el}/

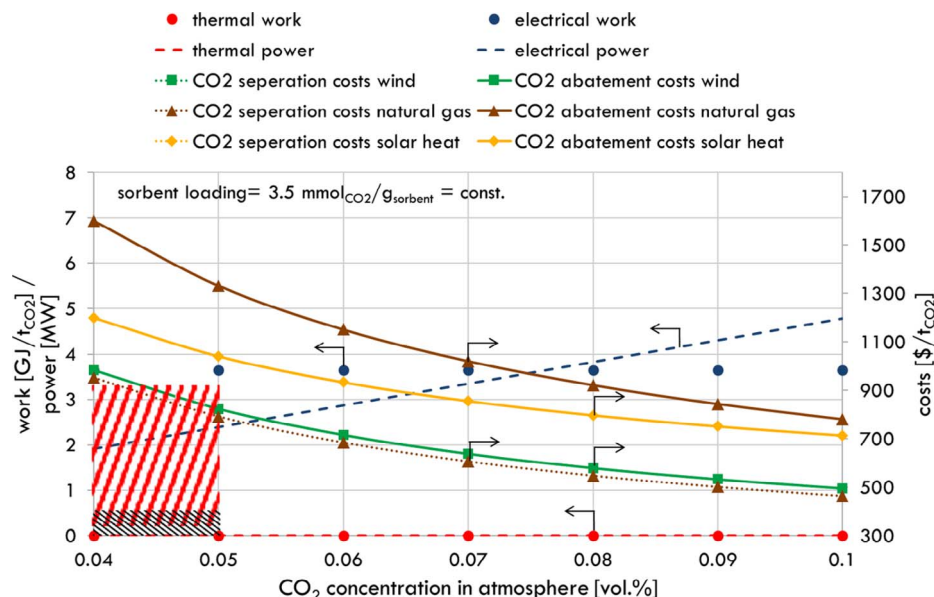


Fig. 7. Energy demand and costs for CO₂ separation from ambient air dependent on the CO₂ concentration (full heat integration assumed).

mol_{CO_2} (Section 4.1). Contrary to this, the necessary electrical power increases from 1.91 MW_{el} at a CO_2 concentration of 0.04 vol.% to 4.78 MW_{el} at 0.1 vol.% because of the larger amounts of CO_2 that must be compressed after separation from the air. The pressure drop does not change, as a constant volume flow of air is assumed for all system calculations. The cost analysis shows that costs decrease with increasing CO_2 concentration, as the high investment costs are related to an increasing amount of separated CO_2 . Three different energy sources were analyzed, namely CO_2 separation powered by natural gas, wind power and solar heat. The dotted lines represent the separation costs; the continuous lines show the values of the abatement costs. The difference between separation costs and abatement costs is defined by Eq. (16):

$$c_A = \frac{c_{PC}}{\tau} \quad (16)$$

In this equation, the abatement costs c_A can be calculated by dividing the specific separation costs c_{PC} by the abatement factor τ , which is defined by Eq. (17):

$$\tau = 1 - \frac{m_{\text{CO}_2, \text{em}}}{m_{\text{CO}_2, \text{sep}}} \quad (17)$$

The abatement factor considers the separated mass of CO_2 , as well as the emitted mass of CO_2 during production of the electrical power needed for the separation process. In the case of fossil fuels like natural gas, the abatement costs significantly differ from the separation costs, because 0.4 $\text{kg}_{\text{CO}_2}/\text{kWh}_{\text{el}}$ are emitted during energy production (combined cycle process, $\tau_{\text{NG}} = 0.59$) [34]. For example, in Fig. 7, the separation costs for a natural gas-driven process are \$ 792/ t_{CO_2} at a CO_2 concentration of 0.05 vol.% in the atmosphere (compare the calculation in Section 4.2). If the amount of emitted CO_2 is considered, the corresponding abatement costs are \$ 1333/ t_{CO_2} . In comparison, the use of renewable energy to power the separation process has clear advantages. Although the separation costs are higher for wind- or solar heat-driven processes than for the natural gas-driven process due to higher energy production costs (the following costs for energy production were assumed: natural gas: \$ 0.061/ kWh_{el} , wind: \$ 0.1/ kWh_{el} , solar heat: \$ 0.3/ kWh_{el} [34]), abatement costs are significantly lower. This effect is most significant at low CO_2 concentrations and diminishes at higher concentrations, because high energy production costs for renewables affect the total costs more significantly with increasing energy demand. As no CO_2 is emitted during energy production with renewable energy, the abatement factor is one and the separation and abatement costs do

not differ. All calculations were conducted with the assumption of a constant sorbent loading of 3.5 $\text{mmol}_{\text{CO}_2}/\text{g}_{\text{sorbent}}$. Still, it must be mentioned that in practice, CO_2 emitted by natural gas power plants would probably be captured directly at the source (CCS) and not from the air. In addition to the costs and work/power needed for the process, data from the literature for amine/imine-based CO_2 separation processes is shown (Fig. 7). The red dashed area shows that the calculated electrical work for other processes from the literature varies between 0.22 $\text{GJ}_{\text{el}}/t_{\text{CO}_2}$ [21] and 3.4 $\text{GJ}_{\text{el}}/t_{\text{CO}_2}$ [32]. As the system described by Zhang et al. provides the basis for the CO_2 separation plant noted here, it is apparent that the calculated electrical work is close to that stated by Zhang et al. [32]. Furthermore, the costs for CO_2 separation from ambient air are depicted by the black dashed area. The costs for this in the literature vary from \$ 30/ t_{CO_2} [33] to \$ 425/ t_{CO_2} [32]. All data from the literature refers to CO_2 concentrations in the atmosphere of 0.04–0.05 vol.%. The costs stated in the literature, however, are far below the values calculated in this contribution. The reasons for the deviation are often overoptimistic assumptions associated with the CO_2 separation systems, such as excessively high component efficiency, low educt prices and the negligence of CO_2 compression after separation, capital costs/investment costs or abatement costs. However, the discrepancy between values from literature and results from this contribution is also related to the specific system design investigated here. Broehm et al. reported a wider cost range from \$ 9.4/ t_{CO_2} to \$ 1200/ t_{CO_2} in their techno-economic analysis [58]. Rajan and Herzog [66] also state possible values of \$ 250/ t_{CO_2} . It must be emphasized that operating and maintenance costs must also be considered. The wide range of estimated and calculated values is caused by a high level of uncertainty and various assumptions. Ishimoto et al. [67] pointed out that the cost certainty in the academic literature is vast; the costs claimed by start-up companies are often lower. In this paper we applied a detailed model which resulted in costs in the upper range.

4.4. Case study 1: separation of global CO_2 emissions

In the first case study, the realization of global CO_2 separation with the described system will be investigated. The results of this will show the point in future the amounts of emitted and separated CO_2 will equalize, how many separation plants need to be erected and what costs this undertaking will entail. It was decided to combine the CO_2 separation plant with renewables, as these have the potential for low abatement costs (as shown in case study 0, Section 4.3). Furthermore,

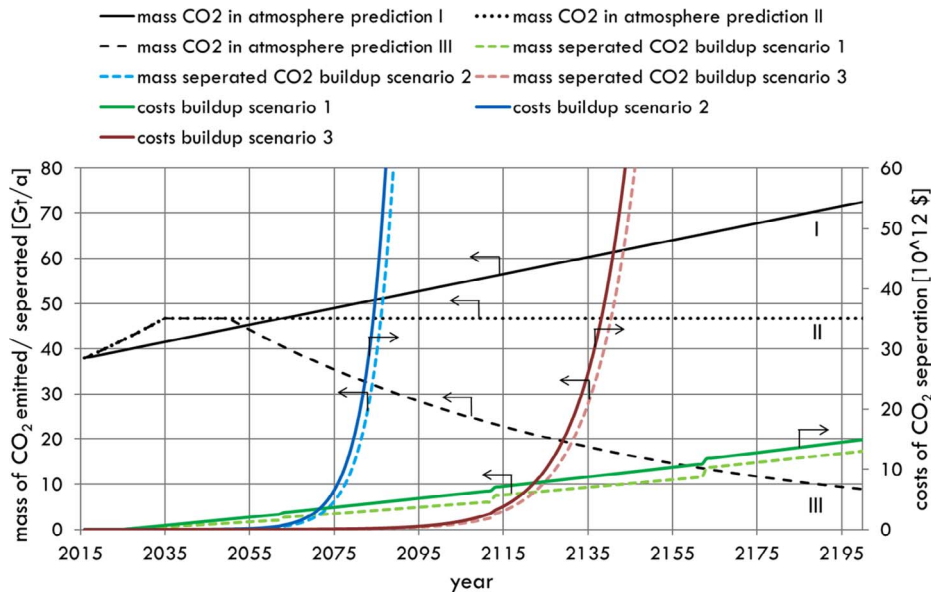


Fig. 8. Case study 1: Scenarios for the separation of global CO_2 emissions.

Table 2Results from case study 1: Overview of buildup scenarios dependent on CO₂ development predictions.

Buildup Scenario 1 (+ 5000 plants/a)	CO ₂ development prediction		
	I (increase)	II (constant)	III (decrease)
Break-even year [–]	–	–	2163
Separation plants [10 ⁶]	–	–	0.7
Costs [10 ¹² \$]	–	–	12
Sahara area [%]	–	–	0.4
Buildup Scenario 2 (+ 20% plants/a)	CO ₂ development prediction		
	I (increase)	II (constant)	III (decrease)
Break-even year [–]	2087	2086	2084
Separation plants [10 ⁶]	3.9	3.3	2.3
Costs [10 ¹² \$]	58	48	34
Sahara area [%]	2.1	1.8	1.2
Buildup Scenario 3 (+ 10% plants/a)	CO ₂ development prediction		
	I (increase)	II (constant)	III (decrease)
Break-even year [–]	2144	2141	2131
Separation plants [10 ⁶]	3.9	2.9	1.1
Costs [10 ¹² \$]	61	46	18
Sahara area [%]	2.1	1.6	0.6

although the energy production costs for solar heat are higher than for wind energy, solar heat was chosen to be combined with the CO₂ separation plant on the basis of the following advantages: the Earth possesses abundant solar energy, solar thermal plants can be built in suitable dimensions to power several CO₂ separation plants, solar thermal plants can be partly operated during the night with suitable energy storage and solar thermal plants can be built in remote locations like deserts where they do not compete for land allocation.

For the example calculations that follow, the Sahara was chosen as a perfect area to erect the CO₂ separation plants in combination with solar heat. The Sahara possesses a huge area of 9400000 km² and a direct normal irradiation (DNI) of approximately 2000–2600 kWh/m²/a [68,69]. As a reference solar thermal power plant, the “Andasol” power plants from southern Spain were selected. The power plant consists of a solar collector field of 0.5 km² and has a capacity of 50 MW_{el} to produce approximately 165 GWh_{el}/a net [70].

In southern Spain, solar irradiation reaches DNI values of approximately 2136 kWh/m²/a, so the Sahara will provide optimal conditions for the solar thermal power plant [70]. For the CO₂ separation plant designed in this paper, with a capacity of 14150 t_{CO2}/a, a land requirement of 600 m² was calculated. The plant design presented here is somewhat better than recent values described by Climeworks [71,72]. Climeworks’ largest facility has a footprint of about 180 m² for a capacity of 1800 t_{CO2}/a. They used an amine-functionalized fibrillated cellulose as adsorbent with a somewhat smaller loading of 1–2 mmol_{CO2}/g_{sorbent} compared to 3.5 mmol_{CO2}/g_{sorbent} assumed for the sorbent in this paper. Advantageously, the direct air capture system designed by Climeworks does not require a cyclone. In addition, as the required electrical work for the separation plant varies between 11.5 and 28.7 GWh_{el}/a net (depending on the CO₂ concentration; calculation here from 0.04 to 0.1 vol.% and 6000 full load hours), approximately ten separation plants can be powered by one “Andasol” solar thermal power plant.

In the following calculations, an additional assumption was that the captured CO₂ can be stored directly in the ground below, so costs for transport do not need to be considered. Furthermore, the following calculations do not account for storage-specific problems such as leakages or limited storage rates or for storage-specific costs for maintenance and observation, etc. Although only a local construction of CO₂ separation plants in the Sahara was considered, it is still possible to deal with global CO₂ emissions. As the air mixture is very efficient throughout the world, no local decrease of CO₂ in the Sahara region will result (as already stated in Section 1). On the other hand, there would

be much higher local CO₂ concentrations close to big emitters like coal power plants [7].

The results of case study 1 are shown in Fig. 8. The three black lines represent three different example scenarios for the development of CO₂ concentrations in future. In scenario I, the amount of emitted CO₂ results from the assumption of a constant increase in CO₂ of 2 ppm/a based on the historical CO₂ trend from 1980 to 2016, described by IPCC [3]. In scenario II, a CO₂ increase of 1.1%/a until 2035 is assumed [73] with a constant amount of emitted CO₂ afterwards. In scenario III, CO₂ first increases at 1.1%/a until 2035 [73]; afterwards, emissions stay constant until 2050 and decrease after that at 1.1%/a. The starting point for all three CO₂ predictions are CO₂ emissions of 38 Gt in 2016. In addition to the three CO₂ evolution predictions, three different system buildup scenarios were calculated. The dotted lines show the amount of separated CO₂ with the number of separation plants erected until a certain point in time. The continuous lines depict the costs associated with the erection of the separation plants and solar thermal power plants. At the point of intersection between the emitted and separated CO₂, it is possible to separate as much CO₂ as is emitted at this point in time. Considering the first buildup scenario, in which an erection rate of 5000 additional separation plants per year is assumed (starting in all buildup scenarios with 50 separation plants in 2025), there is only a break-even point with CO₂ development prediction III in 2163. At that point, 700000 CO₂ separation plants would have been constructed, at a cost of \$ 12 trillion.

In total, 0.4% of the complete Sahara area would have been used for the separation plants and solar thermal power plants (see also Table 2). With buildup scenario 1, it is not possible to reach a break-even point with CO₂ development predictions I and II until 2300 (assumed deadline, not fully shown in Fig. 8). Buildup scenario 2 takes a 20% higher erection rate per year into account, meaning that each year, 20% more CO₂ separation facilities will be built compared to the previous year. As a result, buildup scenario 2 shows an exponential increase in the amount of separated CO₂, as well as in associated cost, because the number of separation plants built increases much faster than in buildup scenario 1.

Break-even points are possible with all three CO₂ development predictions. For example, the break-even year between buildup scenario 2 and CO₂ development prediction I would be 2087. By then, 3.9 million separation plants would have been built and \$ 58 trillion spent in this scenario. In addition, 2.1% of the total Sahara area would have been covered. Further results of buildup scenario 2 with CO₂ development predictions II and III are summarized in Table 2. In the last buildup scenario 3, 10% of the additional separation plants are assumed to be constructed each year. Consequently, break-even points are further in the future (compared to buildup scenario 2), but an intersection is still observable for all three CO₂ development predictions. Depending on the CO₂ development prediction, break-even points are between 2131 and 2144.

A total of 1.1 million to 3.9 million separation plants are necessary to separate as much CO₂ from the atmosphere as is emitted during the specific year and investment ranges between \$ 18 trillion and \$ 61 trillion. The occupied Sahara area varies between 0.6% and 2.1% (see also Table 2). All calculated scenarios show that although plant construction is considered to have already started in 2025, a significant amount of time will be necessary to be able to separate as much CO₂ as will be emitted at a certain point in time in the future. Furthermore, numerous separation plants must be constructed and huge investment is inevitable in any case. The results show that CO₂ separation plants must be constructed exponentially in order to feasibly reach a break-even point between emitted and separated CO₂ in the near future based on the three different CO₂ development predictions investigated. The faster the construction of separation plants proceeds, the earlier we will be able not only to compensate for future CO₂ emissions, but also to reduce the amount of CO₂ in the atmosphere. The results also show that it may be beneficial to apply buildup scenario 3, which has advantages

in terms of cost for CO₂ development predictions II and III compared to buildup scenario 2 (see Table 2). This is due to the fact that the model calculations applied also consider a certain degree of technological improvement in future, which would mean that CO₂ could be separated more cost efficiently (already stated in Section 3.3). It should be noted that the results are only valid for the example of CO₂ development predictions applied here. The calculations do not consider the possibility that potential surplus electrical work from solar thermal power plants could be sold, thus reducing the overall costs, nor do they account for possible future decreases in electricity production costs for solar thermal power plants.

4.5. Case study 2: separation of global CO₂ emissions to achieve the level in 2016

For case study 2, the results from case study 1 were used as the starting point. Then, the number of plants and level of investment required to reduce the CO₂ concentration to the 2016 level was assessed. The motive behind this case study was that it may be important to reduce anthropogenic CO₂ emissions to earlier levels to avoid the hazardous further consequences of climate change. As an example, Fig. 9 shows the results of case study 2 for buildup scenario 2 (20% of additional separation plants/a) with CO₂ development prediction I. The figure shows the difference between CO₂ emitted into the atmosphere (i.e., agglomerated) and the amount separated at a certain point in time.

Until the first break-even point of buildup scenario 2 with CO₂ development prediction I (case study 1, year 2087, see Table 2), a total of 2880 Gt_{CO2} of CO₂ will have agglomerated in the atmosphere. From this point on, it will be possible to remove more CO₂ from the atmosphere than is emitted annually if a further exponential buildup of CO₂ separation plants continues. Fig. 9 shows that a second break-even point is reached in 2101, as the difference between emitted and separated CO₂ decreases exponentially over time. In 2101, the amount of CO₂ is reduced to the concentration of 2016. Fig. 9 also shows the necessary area of the Sahara needed for the separation plants and solar thermal power plants. Approximately 27.3% of the Sahara's total area is needed at the second break-even point, as a total of 51 million CO₂ separation plants will need to have been constructed by this point in time. For this, an investment of \$ 747 trillion would be needed. This amount roughly

Table 3

Results from case study 2: Overview of buildup scenarios dependent on CO₂ development predictions for the reduction of global CO₂ emissions to 2016 levels (Deadline: 2300).

Buildup Scenario 1 (+ 5000 plants/a)	CO ₂ development prediction		
	I (increase)	II (constant)	III (decrease)
Break-even year [–]	–	–	–
Separation plants [10 ⁶]	–	–	–
Costs [10 ¹² \$]	–	–	–
Sahara area [%]	–	–	–
Buildup Scenario 2 (+ 20% plants/a)	CO ₂ development prediction		
	I (increase)	II (constant)	III (decrease)
Break-even year [–]	2101	2101	2100
Separation plants [10 ⁶]	51	51	42
Costs [10 ¹² \$]	747	747	623
Sahara area [%]	27.29	27.29	22.74
Buildup Scenario 3 (+ 10% plants/a)	CO ₂ development prediction		
	I (increase)	II (constant)	III (decrease)
Break-even year [–]	2169	2168	2164
Separation plants [10 ⁶]	42	38	26
Costs [10 ¹² \$]	710	645	441
Sahara area [%]	22.52	20.48	13.99

corresponds to a tenth of global gross domestic product in 2014 [74]. It is therefore very questionable as to whether this would ever be achievable.

The results of the other buildup scenarios and different CO₂ development predictions are summarized in Table 3. When buildup scenario 1 is applied, no second break-even point is achieved before the 2300 deadline. Even with the decreasing CO₂ development prediction III, 1593 t_{CO2} would still remain in the atmosphere in 2300. This result clearly shows that it is essential to exponentially construct CO₂ separation plants for the aggressive removal of CO₂ from the atmosphere. Alongside the scenario depicted in Fig. 9, similar results were also observed for CO₂ development predictions II and III. For prediction II, the break-even year, cost, number of separation plants and requisite Sahara area are identical to CO₂ development prediction I. This is because huge amounts of CO₂ can be separated annually in the future due to the exponential buildup and for both CO₂ development predictions I and II, break-even point can be reached in the same year. Thus, the break-even year for CO₂ development scenario III is also reached in 2100. The

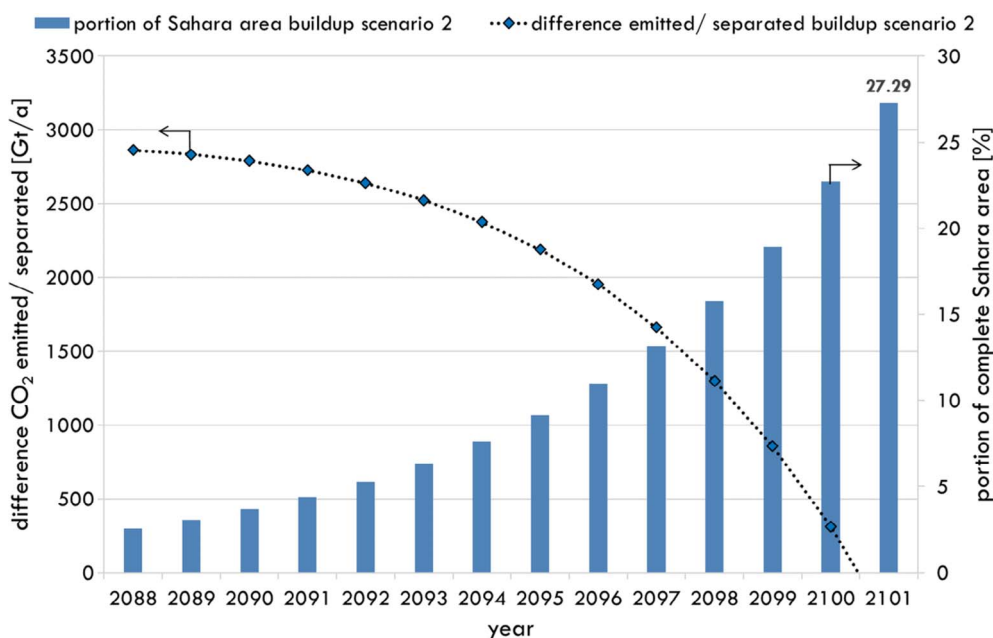


Fig. 9. Case study 2: Results of buildup scenario 2 to reduce the amount of CO₂ to 2016 levels.

associated costs amount to \$ 623 trillion. In this scenario, 42 million CO₂ plants need to be erected, covering 22.7% of the total Sahara area. With regard to buildup scenario 3 (10% additional separation plants/a), break-even years vary between 2164 and 2169, depending on the CO₂ development prediction. This result underlines the fact that higher amounts of CO₂ can be separated earlier in future if the building of the separation plants is accelerated. Between 26 million and 42 million CO₂ separation plants need to be constructed, which will result in costs of \$ 441–710 trillion and a land occupation of approximately 14–22.5% of the total Sahara area.

These results reveal a “quasi contradiction”. For example, “only” 42 million CO₂ separation plants must be erected in buildup scenario 3 to reach the break-even point in 2169 compared to 51 million CO₂ separation plants in buildup scenario 2 to reach the break-even point in 2101 (CO₂ development prediction I is compared), although a lot more CO₂ will have been emitted during the 68 year difference. This results from the assumption (already mentioned above, in Section 4.4) that prospective CO₂ plants will be able to separate more CO₂ at a higher cost efficiency. To summarize, it is obvious that a faster buildup of CO₂ separation plants and lower prospective CO₂ emissions result in an earlier break-even point, in which the amount of CO₂ in the atmosphere can be lowered to the 2016 level. Furthermore, the results show that an exponential buildup is absolutely essential to lower CO₂ emissions to 2016 levels by 2300 and that this exponential buildup causes an insignificant distinction between the break-even years for the different CO₂ development predictions.

4.6. Comparison of CO₂ capture from ambient air and carbon capture and storage (CCS)

In this section, the separation of CO₂ from ambient air is compared to what could be achieved with carbon capture and storage technology (CCS), which might be applied for large local emitters such as coal power plants. As was already stated in Section 1 (Fig. 1), CCS technology may be able to separate approximately 60% of anthropogenic CO₂ emissions. Table 4 compares the three common CCS technologies, namely post-combustion, oxyfuel and pre-combustion. During the post-combustion process, CO₂ with a concentration of approximately 10–15 vol.% in the flue gas is separated after oxidation of the fuel by membranes, or by absorption or adsorption processes.

The oxyfuel process includes cryogenic air separation as an initial step in order to burn the fuel with pure oxygen and enrich CO₂ in the flue gas (ca. 80–98 vol.%), which can then be directly stored afterwards. Cryogenic air separation is also the first step in the pre-combustion process. Oxygen is used to gasify or reform the fuel into hydrogen and carbon monoxide, which is then converted into hydrogen and CO₂ in a water-gas shift reaction. CO₂ at a concentration of > 20 vol.% is again separated by membranes or by absorption or adsorption processes and hydrogen is used as a fuel, only producing water vapor during oxidation [55,56,75,76]. All three technologies feature comparable efficiency drops of 6–14% of the power plant due to the additional electricity demand of the CO₂ separation process. As indicated in Table 4, post-combustion technology offers advantages over oxyfuel and pre-combustion processes, especially in terms of development status, but also partly with respect to complexity and the possibility of changing the setup.

Given these advantages, we decided to compare post-combustion technology with CO₂ separation from ambient air in this paper. As stated by Schiebahn et al. [14], 42 kJ_{el}/mol_{CO2} are needed to separate CO₂ from flue gas during the post-combustion process (30% efficiency was assumed to convert primary energy into electrical work). Compared to the 161 kJ_{el}/mol_{CO2} calculated for the air separation process described in this paper, factor 4 in energy demand can again be found, which was already estimated in thermodynamic calculations (compare Section 1). Regarding the associated costs, Table 4 shows that with the post-combustion process, CO₂ abatement costs might result in \$ 34/t_{CO2}

for a coal-fired power plant and \$ 58/t_{CO2} for a natural-gas-fired power plant, explained in detail by Leung et al. [75]. In the literature, these figures vary widely: abatement costs range between \$ 20/t_{CO2} and \$ 260/t_{CO2} [7,14,16,55,56,75–78]. These costs include transport (liquid or subcritical by, e.g., pipeline, truck, ship, railway) and storage (e.g., aquifers, coal beds, oil/gas reservoirs), amounting to \$ 4.5/t_{CO2}–10 \$/t_{CO2}. Despite the large variation in costs for CCS technology cited in the literature, it is clear that CO₂ separation from ambient air will be much more expensive in any case. The abatement costs for CO₂ separation from ambient air, shown in Table 4, correspond to the base case scenario, also depicted in Fig. 7 (assumption: CO₂ concentration in air: 0.05 vol.%). The abatement costs vary between \$ 824/t_{CO2} for wind-powered separation from air and up to \$ 1333/t_{CO2} for a natural-gas-powered process. There are no costs shown in Table 4 for a coal-powered air separation process because the abatement factor is less than zero. This means that more CO₂ is emitted during the production of the necessary electrical work than can be subsequently extracted from the air by the separation plant. To summarize this comparison, CO₂ separation from ambient air cannot compete with the lower energy demand or with the abatement costs of carbon capture and storage in this direct comparison. As a further argument against CO₂ separation from ambient air, even CCS does not currently offer enough of a financial incentive for widespread commercialization. It should be mentioned, however, that the direct separation of CO₂ from the atmosphere has the potential to separate 100% of CO₂ emissions. Carbon capture and storage can only extract 40–60%.

In a further step, two scenarios will be highlighted to further compare the CO₂ separation costs/abatement costs for CCS and CO₂ separation from the air. In the first scenario, the costs for CO₂ certificates are considered. On the one hand, it is assumed that the CO₂ separation costs/abatement costs for CO₂ separation plants will be reduced by CO₂ certificate costs due to the negative CO₂ balance. On the other hand, CO₂ separation costs/abatement costs for CCS are assumed to increase with the level of the certificate costs due to the higher specific CO₂ emissions (kg_{CO2}/kWh_{el}) caused by the implementation of CCS technology (efficiency decrease). Data for a representative coal power plant with CCS technology can be found in Otto [56]. Otto states 0.1795 t_{CO2em}/t_{CO2sep} for a coal-fired power plant with post-combustion

Table 4

Comparison of carbon capture and storage (CCS) and CO₂ separation from ambient air [7,14,16,55,56,75–78].

	Carbon capture and storage		
	Post-Combustion	Oxyfuel	Pre-Combustion
Efficiency decrease ^a [%]	9–14	7–11	6–11
Energy demand [kJ _{el} /mol _{CO2}]	42		
Status of development	+	–	–
Complexity	+	+	–
Possibility to change setup	+	(+)	–
CO ₂ abatement costs [\$/t _{CO2}]	Coal: 34	Coal: 36	Coal: 23
	Natural gas: 58	Natural gas: 102	Natural gas: 112
	Range literature: 20–260		
CO ₂ transport and storage [\$/t _{CO2}]	4.5–10		
	CO ₂ separation from ambient air		
Energy demand [kJ _{el} /mol _{CO2}]	161		
CO ₂ abatement costs [\$/t _{CO2}]	Coal: –	Natural gas: 1333	Wind: 824
	Solar heat: 1041		

+ = advantage; – = disadvantage; (+) = conditionally applicable/in development.

^a Net efficiency loss incl. CO₂ compression for a coal-fired steam power plant.

capture (MEA absorption). For the CO₂ certificate cost, \$ 40/t_{CO2} were assumed to be valid for 2020 [79]. This will increase by \$ 1/t_{CO2}/a (assumption). The development of the CO₂ separation costs/abatement costs for the CCS coal power plant and CO₂ separation from ambient air – once powered by wind and once by solar heat – is shown in Fig. 10. Due to the refund, CO₂ separation costs/abatement costs decrease linearly for CO₂ separation from ambient air with increasing CO₂ certificate costs. The starting points in Fig. 10 are the above-mentioned \$ 824/t_{CO2} for the wind-powered process and \$ 1041/t_{CO2} for the solar heat-powered process. A constant CO₂ concentration of 0.05 vol.% was assumed for this comparison.

The CO₂ separation/abatement costs increase linearly for coal-fired power plants with post-combustion. Initial CCS CO₂ separation/abatement costs (including transport and storage) of \$ 70/t_{CO2} and \$ 100/t_{CO2} were assumed. Fig. 10 shows a break-even point between CCS and wind-powered CO₂ separation from ambient air with respect to CO₂ abatement costs when CO₂ certificates cost \$ 620/t_{CO2}. As the separation costs are always lower for fossil fuel-fired processes, the break-even point is reached when the CO₂ certificates cost \$ 640/t_{CO2}. If the CO₂ ambient air separation plant is powered by solar heat, CO₂ certificate costs of \$ 800/t_{CO2} and \$ 830/t_{CO2} must be met in order to reach break-even points for abatement costs and separation costs, respectively.

The results show that very high CO₂ certificate costs are needed to achieve cost parity between CCS and CO₂ separation from ambient air. The necessary certificate costs are highly unlikely from today's point of view, as current CO₂ certificate prices are around \$ 5/t_{CO2} and therefore still far below the forecasted costs in [79] for 2020. Furthermore, the CO₂ separation/abatement costs for CCS assumed here are not very optimistic, meaning that even higher CO₂ certificate costs may be necessary to reach cost parity between CCS and CO₂ separation from ambient air.

In the second scenario, the influence of increasing CO₂ concentration in the atmosphere on the cost relation between CCS and CO₂ separation from ambient air is evaluated. The results of this scenario are shown in Fig. 11, which indicates that the costs for CO₂ separation from ambient air decrease less significantly with increasing CO₂ concentration. This effect was already observed in Section 4.3 (Fig. 7) and can be explained by the significant influence of high energy production costs for renewables on the overall costs of the separation process at high CO₂ concentrations. The CO₂ separation/abatement costs for CCS are independent of the CO₂ concentration in the atmosphere. For this

scenario, separation costs of \$ 70/t_{CO2} and abatement costs of \$ 100/t_{CO2} were again assumed, as was a CO₂ certificate price of \$ 100/t_{CO2}.

Fig. 11 shows that it is not possible to reach cost parity between CCS and solar-heat-powered CO₂ separation from ambient air in a CO₂ concentration range of 0.1–0.5 vol.%. In contrast, abatement cost parity between CCS and wind-powered CO₂ separation from ambient air is possible for a CO₂ concentration of 0.45 vol.%. Separation cost parity between CCS and wind-powered CO₂ separation from ambient air is also not possible in the CO₂ concentration range of 0.1–0.5 vol.%. The results show that very high CO₂ concentrations in the atmosphere are necessary to reach cost equilibrium between CCS and CO₂ separation from ambient air. Furthermore, as already stated in Section 1, CO₂ concentrations higher than 0.1 vol.% could already be hygienically harmful to humanity. The scenario considered here is only hypothetical in nature.

The results from this section clearly highlight the disadvantages of CO₂ separation from ambient air in comparison to carbon capture and storage in terms of CO₂ separation/abatement costs. Furthermore, when high CO₂ certificate costs and high CO₂ concentrations in the atmosphere are considered, CO₂ separation from ambient air can only compete with CCS under extraordinary and unrealistic conditions.

4.7. Influence of CO₂ capture from ambient air on production costs

This section evaluates the influence of CO₂ separation from ambient air on the production costs of exemplary industry sectors with high CO₂ emissions. Two cases are considered here: a) a facility of typical plant size that is assumed to compensate for its own CO₂ emissions by installing CO₂ separation plants in the Sahara; and b) CO₂ separation being compulsory for the whole sector, leading to increased production costs.

Table 5 shows CO₂ emissions, production rates and plant sizes for global steel, cement, ethylene and ammonia production. These four products account for the majority of industrial CO₂ emissions. To reduce these CO₂ emissions, carbon capture, utilization and storage (CCUS) process technology is being considered. If the captured carbon is used for fuel production and the origin of carbon is fossil sources, the final CO₂ emissions could be halved in the best case scenario. Another option would be to extract CO₂ from the air as compensation for industrial CO₂ emissions. However, attempts to reduce CO₂ emissions are undermined by increasing production capacities.

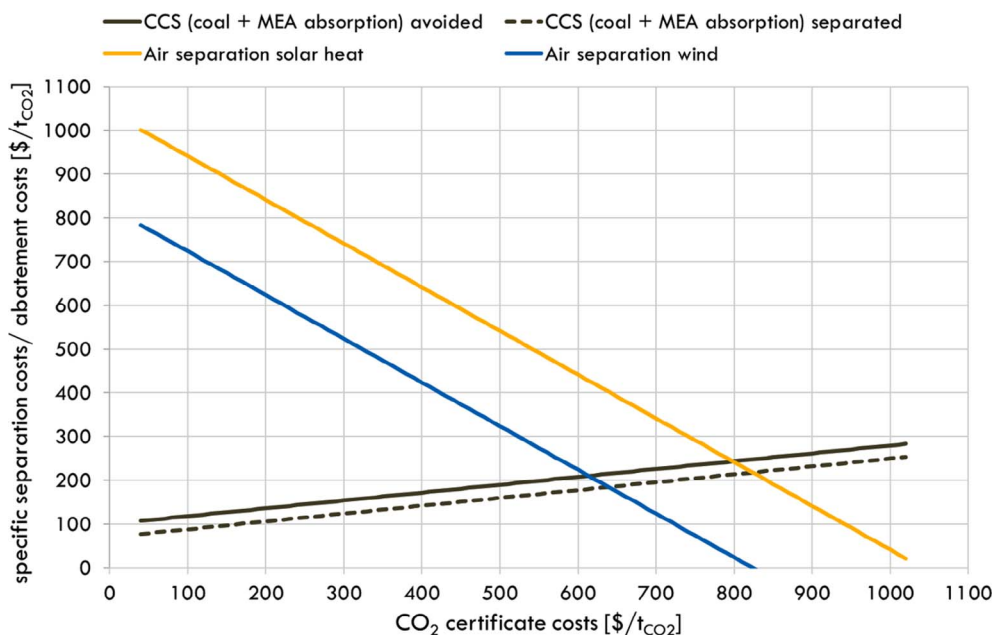


Fig. 10. CO₂ separation/abatement costs for CCS and CO₂ separation from ambient air dependent on the CO₂ certificate cost.

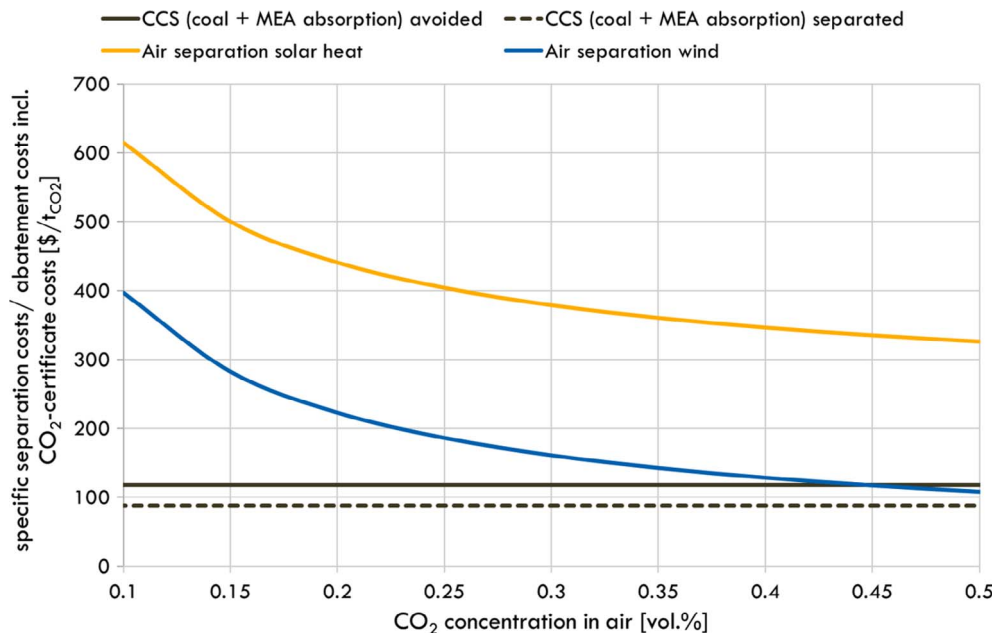


Fig. 11. CO₂ separation/abatement costs, incl. CO₂ certificate costs for CCS and CO₂ separation from ambient air dependent on the CO₂ concentration in the air.

Table 5

CO₂ emissions, production rates and plant sizes for global steel, cement, ethylene and ammonia production.

Category	Unit	Product			
		Cement	Steel	Ethylene	Ammonia
CO ₂ emissions [80] (2002)	Mt/a	928.3	630.0	259.2	112.5
No. of sources [80] (2002)	–	1175	180	240	194
Specific CO ₂ emissions	Mt/a/source	0.79	3.5	1.08	0.58
Production rate (2002)	Mt/a	1946 [86]	905 [87]	75 [82]	107 [84]
Number of separation plants/source	–	56	247	76	41
Investment costs	Bill. \$	2.4	10.7	3.3	1.8
Footprint (Solar)	km ²	2.47	10.93	3.37	1.81
Average Production rate (2013–2015)	Mt/a	4200 [86]	1650 [87]	165 [81]	146 [84]
Price (2002)	\$/t	91.9 [88]	402 [86]	400 [83]	70 [89]
Average price (2013–2015)	\$/t	105.5 [86]	533 [7]	772 [90]	500 [91]

The well-known CO₂ emission data from Gale et al. [80] published in 2005 are based on original data collected in 2002. The production rate of steel nearly doubled in the period 2002–2015, reaching 1650 Mt/a, while the average steel price increased only slightly, from \$ 402/t in 2002 to \$ 533/t averaged between 2013 and 2015. In 2015, the steel price was \$ 413/t, which is comparable to 2002. It should be noted that a maximum of nearly \$ 750/t in 2010 was reached until steel capacities were increased, leading to over-production and a price decrease. Cement production also doubled, to 4200 Mt/a. The average cement price is nearly stable at \$ 100/t, while ethylene production doubled from 75 Mt/a in 2002 to 165 Mt/a in 2015 [81,82]. The ethylene price fluctuated strongly between 1998 and 2012 with a minimum of \$ 250/t in 1990, 1994 and 1999 and maximum of \$ 1500/t in 2008 [83]. The ethylene price depends strongly on crude oil pricing. Ammonia production increased from 107 to 146 Mt/a from 2002 to 2015 [84]. The cost of ammonia fluctuated strongly in the past, with an overall increase from \$ 70 to \$ 500/t averaged between 2013 and 2015.

These figures underline the strong need to develop technologies to reduce CO₂ from industrial production due to the strong increase in average production rates from 2002 to 2015.

If we consider the number of plants noted by Gale et al. [80], specific CO₂ emissions per annum and per source can be calculated [80]. Steel production leads to high emission rates of 3.5 Mt_{CO2}/a/source. This is followed by ethylene and cement with 1.08 and 0.79 Mt_{CO2}/a/source, respectively. Taking the growth in production into account, such as for steel, about 120% related to 2002 on a global basis, improvements in CO₂ emissions of about 20% (such as for steel production in Germany from 1990 to 2015 as an example [85]) cannot compensate for the increasing amount of CO₂. It is not known if higher production capacities can be achieved by expanding plant size or increasing the number of plants. We used the average emission rates determined by Gale et al. [80]. Applying a CO₂ separation plant size with a capacity of 14150 t_{CO2}/a, a total of 56 separation plants are required to compensate for CO₂ emissions from one typical cement production site.

The highest number of separation plants is required for steel production, namely 247 plants for one steel production site. The footprint for direct air capture plants powered by solar energy is 2–11 km² for CO₂ capture, with the lowest footprint for ammonia and highest for steel plants, as indicated in Table 5. Germany's largest steel production site, producing about 8.8 Mt/a, is located in Duisburg on an area of about 10 km² [85]. CO₂ emissions from this facility amount to approximately 12 Mt/a. According to the data in this paper, a direct air capture facility that compensates for these emissions requires a footprint of about 0.5 km² for capture technology and approximately 40 km² for solar electricity production. If wind energy is to be combined with such a capture facility to provide the necessary electrical power which otherwise must come from the grid, about 0.36 GW_{el} would be required for 8000 h of operation per annum. Assuming the installation of wind turbines with 3.5 MW_{el}, a wind park with a minimum of 102 windmills would be required. Further upscaling must be considered due to fewer hours of operation per year at maximum production. At an average of 3000 h of operation per annum with 3.5 MW_{el}, a total of 271 windmills would be required. Additionally, a corresponding storage technology for doldrums would be required for constant operation of the capture facility. These numbers show that direct CO₂ capture from ambient air is not feasible, even for single facilities with high specific CO₂ emissions.

The second case considers CO₂ separation for the entire cement, steel, ethylene and ammonia production sectors. Fig. 12 shows the CO₂ emissions of the different industry sectors per year, as well as the influence on the production costs with and without CO₂ separation from ambient air after emission. A distinction is made between CO₂ separation from ambient air powered by natural gas, solar heat and wind power. Abatement costs for an ambient air CO₂ concentration of 0.05 vol.% were taken into account (natural gas: 1333 \$/t_{CO2}; solar heat: 1041 \$/t_{CO2}; wind power: 824 \$/t_{CO2}). The results show that the subsequent separation of the CO₂ emitted during the specific production processes significantly increases the production costs. The data in Table 5 show that the highest CO₂ emissions are caused by cement production, on the back of its high average production rates. After cement, CO₂ emissions decrease in the order steel, ethylene and ammonia, respectively. Nevertheless, if the specific CO₂ emissions are considered, ethylene accounts for the highest emissions, with 1.57 t_{CO2}/t_{C2H4}. Ethylene is followed by ammonia, steel and cement in terms of specific CO₂ emissions. The results show that for cement, production costs increase from \$ 105.5/t to \$ 287.6/t when CO₂ is separated by a wind-powered direct air separation plant. When the CO₂ separation plant is powered by natural gas, costs increase to \$ 400/t. Consequently, cement production costs increase by a factor of 2.7–3.8 if CO₂ separation becomes compulsory for the cement sector and is realized by direct capture from air. Similar trends can be observed for the other products. Steel production costs increase up to \$ 1042/t (by a factor of 2) when the emitted CO₂ is subsequently captured by natural gas-powered separation plants. For ethylene, production costs increase by up to a factor of 3.7, which results in a price of \$ 2866/t. For ammonia, production costs increase by a factor of 2.3–3.1, amounting to \$ 1527/t when the CO₂ separation plant is powered by natural gas. This brief calculation clearly shows that a drastic increase in production costs is likely to occur for commodities, the production of which is associated with high CO₂ emissions. In parallel, future price development is difficult to predict even without CO₂ separation. During the last 15 years, the prices for ammonia and ethylene strongly increased, while cement was stable at about \$ 100/t. For ammonia, which is extremely important for the fertilizer industry, an increase by a factor of 7 was noted. High fertilizer prices also increase the price of food. In light of these results, much cheaper solutions must be developed and should not be based solely on one technology. In addition, our analysis shows that for small industrial production facilities, a carbon capture plant from air is

not feasible under the prevailing technical conditions.

5. Conclusions and outlook

This paper assessed CO₂ separation from ambient air on a technical and economic level. A system design was proposed based on polyethyleneimine as a sorbent due to its high potential in terms of costs, cyclability, loading and necessary electrical and thermal work. The necessary electrical work to operate the CO₂ separation plant was calculated as 3.65 GJ_{el}/t_{CO2}, which is significantly higher than what is stated in other literature (e.g. 0.36–0.44 GJ_{el}/t_{CO2} [58]). The compression of air and CO₂, as well as the compression demand to overcome pressure losses in the system, are the reasons for the comparably high electrical energy demand. The sum of thermal and electrical energy amounts to 6 GJ/t_{CO2} in the case of heat recuperation. This value is somewhat smaller to the values for most other processes, i.e., 10 GJ/t_{CO2}. If thermal energy is already available as excess heat in the location of interest, then other technology routes with lower electrical energy demands are preferable.

The economic analysis reveals that coupling CO₂ separation from ambient air with renewable energy has the potential to lower CO₂ abatement costs compared to systems powered by fossil fuels. In comparison to the values stated in the literature to date, the calculated specific costs are in the upper range. On the one hand, the reasons for this are often overoptimistic assumptions for CO₂ separation systems in the literature or the negligence of costs. On the other hand, costs are significantly increased by the high electrical energy demand and high component costs of the specific system design investigated in this paper. In two case studies, the separation of the global CO₂ amount was investigated by coupling the separation plants with solar thermal power plants. Different buildup scenarios, in combination with diverse CO₂ development predictions, showed that costs of up to \$ 747 trillion might be needed. This amount corresponds to approximately a tenth of global gross domestic product from 2014. In addition, up to 27.3% of the total Sahara area would be occupied if the number of plants necessary were to be built in this region. Compared to carbon capture and storage (CCS) technology, which can be applied to big point emitters, CO₂ separation from ambient air consumes up to four times more energy and has much higher abatement costs with increases up to a factor of 8–13 (if abatement costs of \$ 100/t_{CO2} are assumed for CCS).

As a general conclusion, the results reported herein show that CO₂

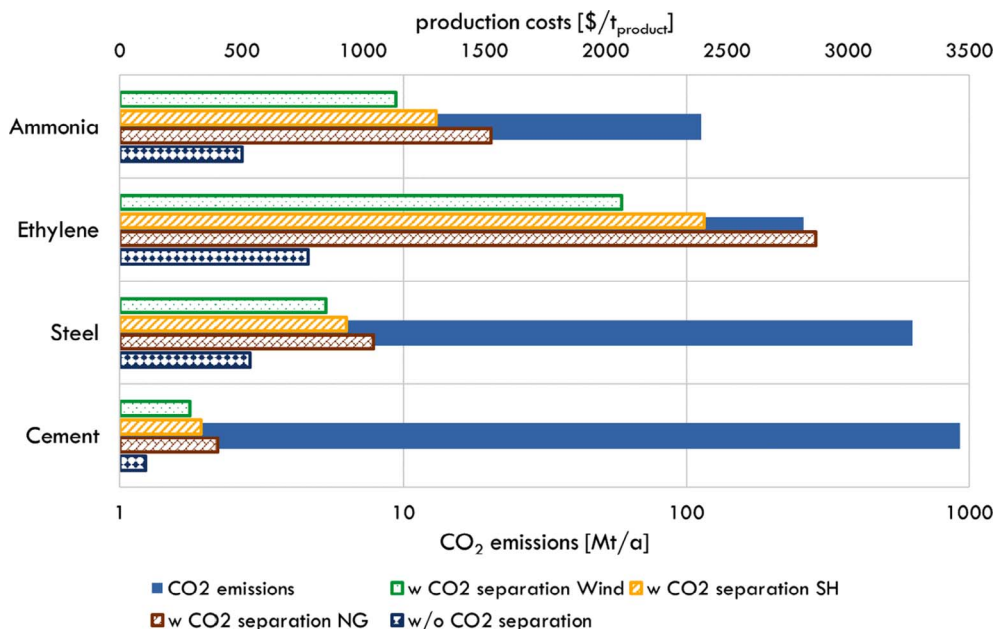


Fig. 12. Influence of the CO₂ separation from ambient air on the production costs of exemplary industry sectors, taken from [7,81–84,86–91].

separation from ambient air will not be able to play a vital role in the abatement of the climate change problem until 2050 due to its strong technological and economic drawbacks. Nevertheless, it must be mentioned that the analysis is based on a specific system design with drawbacks in terms of the electrical energy demand and component costs. To efficiently counteract climate change, a distributed system consisting of technologies to increase the efficiency of the state-of-the-art technology, the substitution of conventional technologies by, e.g., renewable energy and the separation and utilization of CO₂ in power-to-x (PtX) processes, for instance, will be mandatory. In the long term, CO₂ separation from ambient air may still play a vital role in the sequestration of CO₂ from diluted and dispersed sources, to be used afterwards for e.g. fuel production or the production of carbon-based materials. Furthermore, it must be noted that CO₂ separation from ambient air still has the potential for optimization, e.g. by constructing separation plants that use the natural air draft to lower the necessary

electrical work or by applying improved materials (sorbent loading, cyclability, costs, etc.) and efficient system designs.

Finally, the applied methodology in this contribution, including the techno-economic assessment of this new technology route performed, the analysis of its future global impact with case studies, the comparison with competing technology and its possible application in well-known conventional industrial processes, can be applied to the assessment of other new technologies intended to mitigate climate change. In addition, the technical and economic data basis can be used to integrate direct air capture into further applications, such as power-to-x plants.

Acknowledgements

The author expresses special thanks to the fuel processing team at Jülich.

Appendix A

See Tables 6–13.

Table 6
Adsorber parameters, partly taken from [32].

Length (m)	12
Width (m)	12
Height (m)	40
Volume adsorber (m ³)	5760
Air velocity (m/s)	5
Air-adsorbent contact time (s)	8
Flow rate of air (m ³ /s)	720
Adsorption temperature (°C)	20
CO ₂ capture rate (%)	100
Adsorbent working capacity (wt.%)	15
Solid circulating rate (kg/s)	4.37
Solid residence time in bed (min)	15
Inventory bed mass (t)	4
CO ₂ captured in each unit (t/d)	56.61
Size ratio adsorber (m ²)	144

Table 7
Cyclone parameters, partly taken from [32].

Diameter of cyclone (m)	11.20
Height of cyclone (m)	28
Volume cyclone (m ³)	2759
Size ratio cyclone (m ²)	99

Table 8
Desorber parameters, partly taken from [32].

Desorption temperature (°C)	130
Fraction of CO ₂ in stripping gas (%)	0
Fraction of steam in stripping gas (%)	100
Solid residence time in bed (min)	15
Inventory bed mass (t)	4
Diameter of cylindrical desorber (m)	4
Height of desorber (m)	4.80
Volume desorber (m ³)	60.32
Size ratio desorber (m ²)	13

Table 9
Heat exchanger parameters, partly taken from [56].

Heat exchanger surface (m ²)	35.56
Logarithmic mean temperature difference (K)	328.15
Heat transmission coefficient (W/m ² /K)	70

Table 10
Evaporator parameters, partly taken from [56].

Heat exchanger surface (m ²)	3.11
Logarithmic mean temperature difference (K)	328.15
Heat transmission coefficient (W/m ² /K)	1700

Table 11
Condenser parameters, partly taken from [56].

Heat exchanger surface (m ²)	4.11
Logarithmic mean temperature difference (K)	328.15
Heat transmission coefficient (W/m ² /K)	1200

Table 12
Component-specific coefficients K_1 , K_2 , K_3 and Z for the economic analysis, taken from [56].

Component	Description	K_1	K_2	K_3	Z
Adsorber	Reactor with jacket	3.3496	0.7235	0.0025	5760 m ³
Desorber	Reactor with jacket	3.3496	0.7235	0.0025	60.32 m ³
Evaporator	Forced circulation	5.0238	0.3475	0.0703	3.11 m ²
Heat Exchanger	Bundled tubes	4.3247	−0.303	0.1634	35.56 m ²
Condenser	Forced circulation	5.0238	0.3475	0.0703	4.11 m ²
Cyclone	Vertical vessel	3.4974	0.4485	0.1074	2759 m ³
Compressor 1	Radial, axial, piston	2.2897	1.3604	−0.1027	1965.2 kW
Compressor 2	Radial, axial, piston	2.2897	1.3604	−0.1027	425.5 kW
E-motor 1	Closed motor	1.956	1.7142	−0.2282	2183.5 kW
E-motor 2	Closed motor	1.956	1.7142	−0.2282	472.8 kW

Table 13
Component specific coefficients B_1 , B_2 , F_M , F_P or F_{BM} for the economic analysis, taken from [56].

Component	Description	$F_{BM} = B_1 + B_2$		$F_{BM} = F_M * F_P$
		B_1	B_2	
Adsorber	Reactor with jacket			4.00
Desorber	Reactor with jacket			4.00
Evaporator	Forced circulation			2.90
Heat Exchanger	Bundled tubes	1.63	1.66	
Condenser	Forced circulation			2.90
Cyclone	Vertical vessel	2.25	1.82	
Compressor 1	Radial, axial, piston			3.80
Compressor 2	Radial, axial, piston			3.80
E-motor 1	Closed motor			1.50
E-motor 2	Closed motor			1.50

References

- [1] Titus JG. Greenhouse effect and global warming. In: Schwartz ML, editor. Encyclopedia of coastal science. Dordrecht (Netherlands): Springer; 2005. p. 494–501.
- [2] Arrhenius SXXXI. On the influence of carbonic acid in the air upon the temperature of the ground. Lond Edinburgh Dublin Philos Mag J Sci. 1896;41:237–76.
- [3] Climate change 2014: synthesis report. Contribution of working groups I, II and III to the fifth assessment report of the intergovernmental panel of climate change. In: Core Writing Team, Pachauri RK, Meyer LA, editors. Geneva (Switzerland): IPCC; 2014. p. 15.
- [4] Trends in atmospheric carbon dioxide: recent monthly average Mauna Loa CO₂. U. S. Department of Commerce, National Oceanic and Atmospheric Administration, Earth System Research Laboratory, Global Monitoring Division; 2017. < <https://www.esrl.noaa.gov/gmd/ccgg/trends/#globa> > [access Date: 22.08.2017].
- [5] Climate change 1995. The science of climate change. In: Houghton JT, Meira Filho LG, Callander BA, Harris N, Kattenberg A, Maskell K, editors. Contribution of WGI to the second assessment report of the intergovernmental panel of climate change. IPCC: Cambridge (New York), Melbourne; 1996. p. 588.
- [6] Pham T-H, Lee B-K, Kim J, Lee C-H. Enhancement of CO₂ capture by using synthesized nano-zeolite. J Taiwan Inst Chem Eng 2016;64:220–6.
- [7] Goepfert A, Czaun M, Surya Prakash GK, Olah GA. Air as the renewable carbon source of the future: an overview of CO₂ capture from the atmosphere. Energy Environ Sci 2012;5:7833.
- [8] Field CB, Mach KJ. Rightsizing carbon dioxide removal. Science 2017;356:706–7.
- [9] Senftle TP, Carter EA. The holy grail: chemistry enabling an economically viable CO₂ capture, utilization, and storage strategy. Acc Chem Res 2017;50:472–5.
- [10] Wilcox J, Psarras PC, Liguori S. Assessment of reasonable opportunities for direct air capture. Environ Res Lett 2017;12:065001.
- [11] Patel HA, Byun J, Yavuz CT. carbon dioxide capture adsorbents: chemistry and methods. ChemSusChem 2017;10:1303–17.
- [12] Zhang X, Bauer C, Mutel CL, Volkart K. Life cycle assessment of power-to-gas: approaches, system variations and their environmental implications. Appl Energy 2017;190:326–38.
- [13] Parra D, Zhang X, Bauer C, Patel MK. An integrated techno-economic and life cycle environmental assessment of power-to-gas systems. Appl Energy 2017;193:440–54.
- [14] Schiebahn S, Grube T, Robinius M, Zhao L, Otto A, Kumar B, et al. Power to gas.

- Transition to renewable energy systems. Wiley-VCH Verlag GmbH & Co. KGaA; 2013. p. 813–48.
- [15] Socolow R, Desmond M, Aines R, Blackstock J, Bolland O, Kaarsberg T, et al. Direct air capture of CO₂ with chemicals: a technology assessment for the APS panel on public affairs. *APS Phys* 2011:100.
 - [16] House KZ, Baclig AC, Ranjan M, van Nierop EA, Wilcox J, Herzog HJ. Economic and energetic analysis of capturing CO₂ from ambient air. *Proc Natl Acad Sci USA* 2011;108:20428–33.
 - [17] Koytsoumpa EI, Bergins C, Kakaras E. The CO₂ economy: review of CO₂ capture and reuse technologies. *J Supercrit Fluids* 2018;132:3–16.
 - [18] Choi S, Drese JH, Eisenberger PM, Jones CW. Application of amine-tethered solid sorbents for direct CO₂ capture from the ambient air. *Environ Sci Technol* 2011;45:2420–7.
 - [19] Belmabkhout Y, Serna-Guerrero R, Sayari A. Amine-bearing mesoporous silica for CO₂ removal from dry and humid air. *Chem Eng Sci* 2010;65:3695–8.
 - [20] Choi S, Gray ML, Jones CW. Amine-tethered solid adsorbents coupling high adsorption capacity and regenerability for CO₂ capture from ambient air. *ChemSusChem* 2011;4:628–35.
 - [21] Wurzbacher JA, Gebald C, Piatkowski N, Steinfeld A. Concurrent separation of CO₂ and H₂O from air by a temperature-vacuum swing adsorption/desorption cycle. *Environ Sci Technol* 2012;46:9191–8.
 - [22] Gebald C, Wurzbacher JA, Tingaut P, Zimmermann T, Steinfeld A. Amine-based nanofibrillated cellulose as adsorbent for CO(2) capture from air. *Environ Sci Technol* 2011;45:9101–8.
 - [23] Wurzbacher JA, Gebald C, Steinfeld A. Separation of CO₂ from air by temperature-vacuum swing adsorption using diamine-functionalized silica gel. *Energy Environ Sci* 2011;4:3584.
 - [24] Stuckert NR, Yang RT. CO₂ capture from the atmosphere and simultaneous concentration using zeolites and amine-grafted SBA-15. *Environ Sci Technol* 2011;45:10257–64.
 - [25] Didas SA, Kulkarni AR, Sholl DS, Jones CW. Role of amine structure on carbon dioxide adsorption from ultradilute gas streams such as ambient air. *ChemSusChem* 2012;5:2058–64.
 - [26] Wang X, Ma X, Schwartz V, Clark JC, Overbury SH, Zhao S, et al. A solid molecular basket sorbent for CO₂ capture from gas streams with low CO₂ concentration under ambient conditions. *PCCP* 2012;14:1485–92.
 - [27] Sakwa-Novak MA, Jones CW. Steam induced structural changes of a poly(ethyleneimine) impregnated gamma-alumina sorbent for CO₂ extraction from ambient air. *ACS Appl Mater Interf* 2014;6:9245–55.
 - [28] Alkhabbaz MA, Bollini P, Foo GS, Sievers C, Jones CW. Important roles of enthalpic and entropic contributions to CO₂ capture from simulated flue gas and ambient air using mesoporous silica grafted amines. *J Am Chem Soc* 2014;136:13170–3.
 - [29] Goepfert A, Czaun M, May RB, Prakash GK, Olah GA, Narayanan SR. Carbon dioxide capture from the air using a polyamine based regenerable solid adsorbent. *J Am Chem Soc* 2011;133:20164–7.
 - [30] Goepfert A, Meth S, Prakash GKS, Olah GA. Nanostructured silica as a support for regenerable high-capacity organoamine-based CO₂ sorbents. *Energy Environ Sci* 2010;3:1949.
 - [31] Chaikittisilp W, Kim H-J, Jones CW. Mesoporous alumina-supported amines as potential steam-stable adsorbents for capturing CO₂ from simulated flue gas and ambient air. *Energy Fuel* 2011;25:5258–37.
 - [32] Zhang W, Liu H, Sun C, Drage TC, Snape CE. Capturing CO₂ from ambient air using a polyethyleneimine-silica adsorbent in fluidized beds. *Chem Eng Sci* 2014;116:306–16.
 - [33] Lackner KS. Capture of carbon dioxide from ambient air. *Eur Phys J Spec Top* 2009;176:93–106.
 - [34] Kulkarni AR, Sholl DS. Analysis of equilibrium-based TSA processes for direct capture of CO₂ from air. *Ind Eng Chem Res* 2012;51:8631–45.
 - [35] Chaikittisilp W, Lunn JD, Shantz DF, Jones CW. Poly(L-lysine) brush-mesoporous silica hybrid material as a biomolecule-based adsorbent for CO₂ capture from simulated flue gas and air. *Chem – Eur J* 2011;17:10556–61.
 - [36] Gebald C, Wurzbacher JA, Steinfeld A. Amine containing fibrous structure for adsorption of CO₂ from atmospheric air. In: Office EP, editor. B01D 53/04 ed. Switzerland; 2010. p. 28.
 - [37] Nikulshina V, Hirsch D, Mazzotti M, Steinfeld A. CO₂ capture from air and co-production of H₂ via the Ca(OH)₂–CaCO₃ cycle using concentrated solar power—thermodynamic analysis. *Energy* 2006;31:1715–25.
 - [38] Nikulshina V, Gálvez ME, Steinfeld A. Kinetic analysis of the carbonation reactions for the capture of CO₂ from air via the Ca(OH)₂–CaCO₃–CaO solar thermochemical cycle. *Chem Eng J* 2007;129:75–83.
 - [39] Nikulshina V, Gebald C, Steinfeld A. CO₂ capture from atmospheric air via consecutive CaO-carbonation and CaCO₃-calcination cycles in a fluidized-bed solar reactor. *Chem Eng J* 2009;146:244–8.
 - [40] Nikulshina V, Steinfeld A. CO₂ capture from air via CaO-carbonation using a solar-driven fluidized bed reactor—effect of temperature and water vapor concentration. *Chem Eng J* 2009;155:867–73.
 - [41] Matthews L, Lipiński W. Thermodynamic analysis of solar thermochemical CO₂ capture via carbonation/calcination cycle with heat recovery. *Energy* 2012;45:900–7.
 - [42] Keith DW, Ha-Duong M, Stolaroff JK. Climate strategy with CO₂ capture from the air. *Clim Change* 2005;74:17–45.
 - [43] Heidel K, Keith D, Singh A, Holmes G. Process design and costing of an air-contactor for air-capture. *Energy Proc* 2011;4:2861–8.
 - [44] Baciocchi R, Storti G, Mazzotti M. Process design and energy requirements for the capture of carbon dioxide from air. *Chem Eng Process Process Intensif* 2006;45:1047–58.
 - [45] Zeman F. Energy and material balance of CO₂ capture from ambient air. *Environ Sci Technol* 2007;41:7558–63.
 - [46] Stolaroff JK, Keith DW, Lowry GV. Carbon dioxide capture from atmospheric air using sodium hydroxide spray. *Environ Sci Technol* 2008;42:2728–35.
 - [47] Veselovskaya JV, Derevchikov VS, Kardash TY, Stokus OA, Trubitsina TA, Okunev AG. Direct CO₂ capture from ambient air using K₂CO₃/Al₂O₃ composite sorbent. *Int J Greenhouse Gas Control* 2013;17:332–40.
 - [48] Derevchikov VS, Veselovskaya JV, Kardash TY, Trubitsyn DA, Okunev AG. Direct CO₂ capture from ambient air using K₂CO₃/Y₂O₃ composite sorbent. *Fuel* 2014;127:212–8.
 - [49] Polak RB, Steinberg M. Carbon dioxide removal systems. In: Office USPat, editor. US: Coaway LLC; 2012. p. 20.
 - [50] Hofmann H, Baerns M, Renken A. *Chemische Reaktionstechnik*. 3., durchges. Aufl. ed Weinheim: Wiley-VCH; 2002.
 - [51] NIST chemistry webbook. NIST standard reference database number 69. Gaithersburg (MD): National Institute of Standards and Technology.
 - [52] Klotz IM, Rosenberg RM. *Chemical thermodynamics*. 5th ed. New York: Jon Wiley & Sons; 1994.
 - [53] Smith JM, van Ness HC. *Introduction to chemical engineering thermodynamics*, 4th ed. McGraw-Hill; 1987.
 - [54] Hartmann N, Vöhringer O, Kruck C, Eltrop L. Simulation and analysis of different adiabatic compressed air energy storage plant configurations. *Appl Energy* 2012;93:541–8.
 - [55] Nazarko Y. *Energetische und wirtschaftliche Optimierung eines membranbasierten Oxyfuel-Dampfkraftwerkes*. Jülich: Forschungszentrum Jülich GmbH, Zentralbibliothek, Verlag; 2015.
 - [56] Otto A. *Chemische, verfahrenstechnische und ökonomische Bewertung von Kohlendioxid als Rohstoff in der chemischen Industrie*. Jülich (Germany): Forschungszentrum Jülich GmbH, Zentralbibliothek, Verlag; 2015.
 - [57] Linnhoff B. Pinch technology for the synthesis of optimal heat and power-systems. *J Energy Resour Technol-Trans ASME* 1989;111:137–47.
 - [58] Techno-economic review of direct air capture systems for large scale mitigation of atmospheric CO₂; 2015.
 - [59] Garrett DE. *Chemical engineering economics*. Van Nostrand Reinhold; 1989.
 - [60] Polyethylenimine, polyethylenimine suppliers and manufacturers at Alibaba.com.; 2018. < <https://www.alibaba.com/showroom/polyethylenimine.html> > [access date: 31.01.2018].
 - [61] Schmidt S, Moser P. CO₂ Abtrennung mit Monoethanolamin für braunkohle-gefeuerte Kraftwerke. *VGB PowerTech* 2013;12:35–41.
 - [62] Moser P, Schmidt S, Wallus S, Ginsberg T, Sieder G, Clausen I, et al. Enhancement and long-term testing of optimised post-combustion capture technology—results of the second phase of the testing programme at the Niederaussem pilot plant. *Energy Proc* 2013;37:2377–88.
 - [63] Moser P, Schmidt S, Stahl K. Investigation of trace elements in the inlet and outlet streams of a MEA-based post-combustion capture process results from the test programme at the Niederaussem pilot plant. *Energy Proc* 2011;4:473–9.
 - [64] Moser P, Schmidt S, Sieder G, Garcia H, Stoffregen T, Stamatov V. The post-combustion capture pilot plant Niederaussem—results of the first half of the testing programme. *Energy Proc* 2011;4:1310–6.
 - [65] Moser P, Wiechers G, Stahl K, Stoffregen T, Vorberg G, Lozano GA. Ergebnisse des zehnjährigen Entwicklungsprogramms von BASF, Linde und RWE Generation an der CO₂-Wäsche-Pilotanlage in Niederaußem – OASE blue: 2,5 GJ/tCO₂, < 300 gWaschmittel/tCO₂, effektive Emissionskontrolle. 49 Kraftwerkstechnisches Kolloquium, Dresden; 2017.
 - [66] Ranjan M, Herzog HJ. Feasibility of air capture. *Energy Proc* 2011;4:2869–76.
 - [67] Ishimoto Y, Sugiyama M, Kato E, Moriyama R, Tsuzuki K, Kurosawa A. Putting costs of direct air capture in context FCEA working paper series: 002; 2017.
 - [68] Huld T, Müller R, Gambardella A. A new solar radiation database for estimating PV performance in Europe and Africa. *Sol Energy* 2012;86:1803–15.
 - [69] Xu X, Vignaroban K, Xu B, Hsu K, Kannan AM. Prospects and problems of concentrating solar power technologies for power generation in the desert regions. *Renew Sustain Energy Rev* 2016;53:1106–31.
 - [70] The parabolic trough power plants Andasol 1 to 3. The largest solar plants in the world - Technology premiere in Europe; 2011.
 - [71] CLIMEWORKS CO₂ capture plant. Climeworks; 2017. < <http://www.climeworks.com/our-products/> > [24.08.2017].
 - [72] Gebald C, Piatkowski N, Wurzbacher JA. Steam assisted vacuum desorption process for carbon dioxide capture. In: AG C, editor. Espacenet; 2016.
 - [73] CO₂-Ausstoß steigt jährlich um 1,1 Prozent. Spiegel online; 2014. < <http://www.spiegel.de/wissenschaft/mensch/energieerzeugung-co2-ausstoss-steigt-jaehrlich-um-1-1-prozent-a-972843.html> > [access Date: 22.01.2018].
 - [74] Global GDP (gross domestic product) at current prices from 2010 to 2020 (in billion U.S. dollars) Statista; 2017. < <https://www.statista.com/statistics/268750/global-gross-domestic-product-gdp/> > [access date: 04.05.2017].
 - [75] Leung DYC, Caramanna G, Maroto-Valer MM. An overview of current status of carbon dioxide capture and storage technologies. *Renew Sustain Energy Rev* 2014;39:426–43.
 - [76] Schiebahn ST. *Effizienzoptimierte CO₂-Abtrennung in IGCC-Kraftwerken mittels Wassergas-Shift-Membranreaktoren*. Jülich: Forschungszentrum Jülich GmbH, Zentralbibliothek, Verlag; 2014.
 - [77] Jones N. Climate crunch-sucking it up. *Nature* 2009;458:1094–7.
 - [78] Pritchard C, Yang A, Holmes P, Wilkinson M. Thermodynamics, economics and systems thinking: what role for air capture of CO₂? *Process Saf Environ Prot* 2015;94:188–95.
 - [79] Kosten und Potenziale der Vermeidung von Treibhausgasemissionen in Deutschland. Eine Studie von McKinsey & Company, Inc., erstellt im Auftrag von

- BDI initiativ – Wirtschaft für Klimaschutz. McKinsey & Company, Inc.; 2007. p. 70.
- [80] Gale J, Bradshaw J, Chen Z, Garg A, Gomez D, Rogner H-H, et al. Sources of CO₂. In: Metz B, Davidson O, Coninck Hd, Loos M, Meyer L, editors. Carbon dioxide capture and storage. Cambridge: Intergovernmental Panel on Climate Change; 2005. p. 431.
- [81] Aramo M. Global ethylene market outlook. Inaugural ethylene forum; 2015.
- [82] Carty DM, Mullen P. Lummus technology. In: CB&I, editor. CB&I Investor/Analyst Day. CB&I; 2011.
- [83] LTD. DSAP. Ethylene price history and trends. Duncan Seddon & Associates PTY. LTD.; 2012.
- [84] Apodaca LE. Nitrogen fixed–ammonia. Mineral commodity summaries. U.S. Geological Survey; 2016.
- [85] Fakten Stahlindustrie 2016. In: Stahl W, editor. Düsseldorf: Wirtschaftsvereinigung Stahl; 2016.
- [86] Index zur Eisen- und Stahlpreisentwicklung* in Deutschland in den Jahren 2000 bis 2016 (2010 = Index 100). Statista; 2017. < <https://de.statista.com/statistik/daten/studie/377846/umfrage/stahlpreisentwicklung-in-deutschland/> > [19.6.2017].
- [87] association Ws. World steel in figures 2016. Brussels: World steel association; 2016. p. 17.
- [88] Oss HGv. cement. US Geological Survey Minerals Yearbook; 2002.
- [89] Kohn R. Prices and market concentration in the fertilizer industry. In: news Fs, editor; 2015.
- [90] Lippe D. Infrastructure issues slow first-half 2015 ethylene production. Oil Gas J 2015.
- [91] Peters R. Der Ausblick auf den Stickstoff- und Phosphormarkt 2014/2015. Pflanzenschutz- und Düngemittelhandelstag. Burg Warenberg; 2014.
- [92] IEA. CO₂ emissions from fuel combustion. OECD Publishing; 2015.